

A margin-based replacement for cross-entropy loss

Michael W. Spratling
Heiko H. Schütt

michael.spratling@uni.lu
heiko.schutt@uni.lu

University of Luxembourg, Department of Behavioural and Cognitive Sciences, L-4366 Esch-sur-Alzette, Luxembourg.

Abstract

Cross-entropy (CE) loss is the de-facto standard for training deep neural networks to perform classification. However, CE-trained deep neural networks struggle with robustness and generalisation issues. To alleviate these issues, we propose high error margin (HEM) loss, a variant of multi-class margin loss that overcomes the training issues of other margin-based losses. We evaluate HEM extensively on a range of architectures and datasets. We find that HEM loss is more effective than cross-entropy loss across a wide range of tasks: unknown class rejection, adversarial robustness, learning with imbalanced data, continual learning, and semantic segmentation (a pixel-level classification task). Despite all training hyper-parameters being chosen for CE loss, HEM is inferior to CE only in terms of clean accuracy and this difference is insignificant. We also compare HEM to specialised losses that have previously been proposed to improve performance on specific tasks. LogitNorm, a loss achieving state-of-the-art performance on unknown class rejection, produces similar performance to HEM for this task, but is much poorer for continual learning and semantic segmentation. Logit-adjusted loss, designed for imbalanced data, has superior results to HEM for that task, but performs more poorly on unknown class rejection and semantic segmentation. DICE, a popular loss for semantic segmentation, is inferior to HEM loss on all tasks, including semantic segmentation. Thus, HEM often out-performs specialised losses, and in contrast to them, is a general-purpose replacement for CE loss.

Keywords: deep learning; loss functions; robustness; generalisation; image classification; imbalanced data; continual learning; semantic segmentation

Code: <https://codeberg.org/mwspratling/HEMLoss>

1 Introduction

Deep neural networks (DNNs) are generally trained using variants of stochastic gradient descent. These optimisation techniques require the loss function to have a gradient. This means that we are prevented from maximising the classification accuracy directly as this function is piece-wise constant, and therefore, does not define a usable gradient. As a result, for classification tasks it is necessary to use an alternative (“surrogate”) loss function that has a gradient and that still encourages few classification errors. There are potentially many loss functions that meet these requirements, and different choices will change both the speed of training and the parameters training converges to. However, cross-entropy (CE) loss is by far the most common choice as it typically trains classifiers that perform accurately on many different tasks.

In some specific domains better performance can be obtained by using other losses. For example, alternative losses and regularisation terms have been proposed to improve robustness to adversarial attack (Awasthi et al., 2023; Cui et al., 2024; Kanai et al., 2023; Kannan et al., 2018; Mao et al., 2019; Pang et al., 2020; Panum et al., 2021; Tack et al., 2022; Yu and Xu, 2023; Zhang et al., 2019). In the domain of open-set recognition, where the aim is to better detect and reject images from “unknown” classes, alternative losses (such as contrastive losses) have been employed together with architectural modifications to improve performance beyond that achieved by CE (Ming et al., 2023; Zhu et al., 2023). Alternatively, LogitNorm loss (Wei et al., 2022), can be employed to improve unknown class rejection without the need for modifications to the network architecture or training procedure. To deal with situations where the training data contains drastically different numbers of samples for different classes (“class imbalance”), state-of-the-art approaches use a logit-adjusted loss which weights minority classes more heavily (Cui et al., 2019; Menon et al., 2021; Ren et al., 2020). For semantic segmentation, where the aim is to assign a class label to each image pixel, the two largest groups of losses centre around cross-entropy loss and its variants, and DICE loss and its variants (Azad et al., 2023; Ma et al., 2021). DICE loss (Milletari et al., 2016) is designed to be particularly effective when there is class imbalance, a common situation in segmentation tasks. While these specialised losses can outperform cross-entropy loss on the specific tasks for which they were developed, they tend to perform poorly outside of their specialised domain, as is confirmed by our results which are summarised in Fig. 1.

The fact that specialised losses out-perform cross-entropy on certain tasks motivates the search for a better classification loss function, that can perform well on a range of tasks (*i.e.*, is general-purpose, rather than specialised). For simpler statistical models, margin based losses are known to show better generalisation behaviour (Crammer and Singer, 2002). We thus hypothesised that a margin-based loss should have advantageous properties compared to CE loss (as discussed in detail in Section 2). Particularly, we expected a margin-based loss to train networks that were less susceptible to making over-confident predictions, and hence, that would be better able to distinguish known from unknown classes. Furthermore, we expected a margin-based loss to be less prone to over-writing previously learnt weights, and hence, be less susceptible to catastrophic forgetting in continuous learning and less prone to weights appropriate for the majority classes over-writing those for minority classes when training with imbalanced data. Hence, a margin-based loss is a promising candidate for a good general purpose classification loss function. However, the existing Multi-class Margin (MM) loss trains DNNs that have

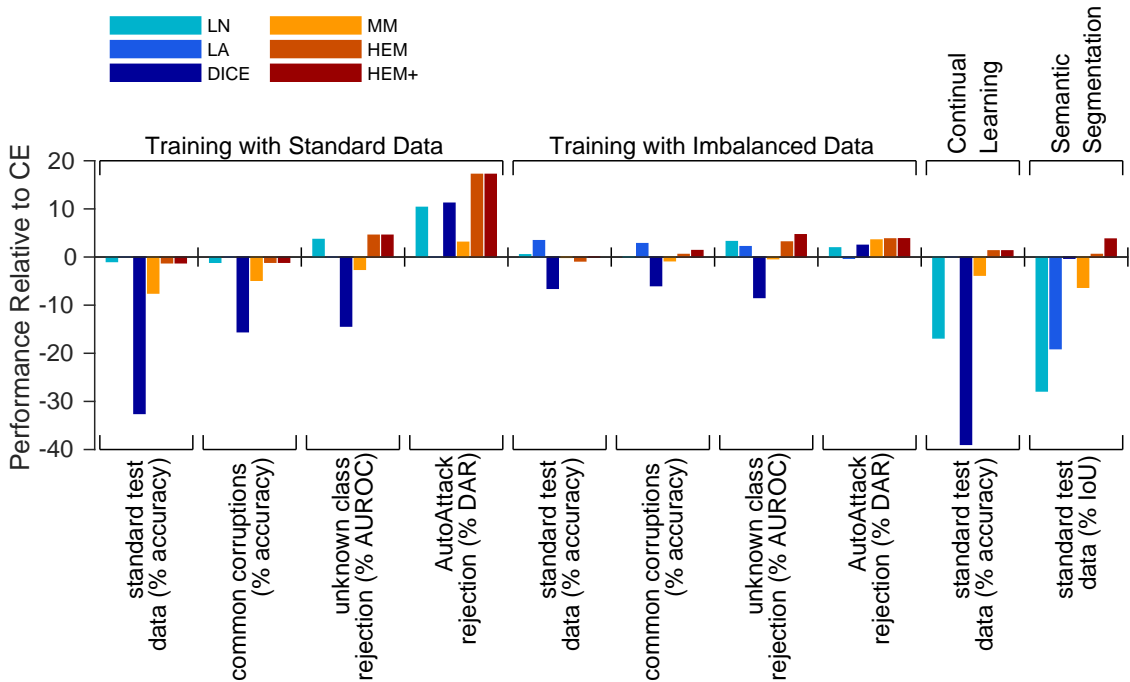


Figure 1: Summary results for all the different tasks considered, comparing the average performance of cross-entropy (CE) loss to each of the alternative losses that have been evaluated: LogitNorm (LN), Logit-adjusted (LA), DICE, multi-class margin (MM), high error margin (HEM), and high error margin with adjusted margins (HEM+). Results are averaged using the arithmetic mean over all other factors that were varied in the experiments, such as data-set and network architecture. For all the evaluation metrics used, higher values indicate better performance. The relative performance is calculated by subtracting the performance produced by CE loss from the corresponding metric for each of the other losses. Hence, positive values indicate performance better than that of CE loss. Note that the results for LA are equal to those of CE, and the results for HEM+ are equal to those of HEM when the training data is balanced (*i.e.*, when using standard training data and performing continual learning).

performance that is not competitive with CE loss (Fig. 1). We propose a fix for these training problems which yields a loss that generally works better than cross-entropy loss.

In Section 2 we identify issues with both CE and MM losses. Based on this analysis, we propose the high error margin (HEM) loss, a variant of Multi-class Margin loss that overcomes the training issues that have previously prevented margin-based losses from training high-performing DNNs (Section 4). In extensive evaluations performed using more than eighteen different neural network architectures and eight different data-sets (ranging in size from MNIST to ImageNet1k), we show that HEM is competitive with or out-performs cross-entropy loss across a range of classification tasks (Section 5).

2 Analysis and Motivation

To motivate our new loss, we first describe shortcomings of CE loss and discuss how a margin based loss may fix those shortcomings. Then we describe the issues with MM loss, the current margin-based loss. Our method for addressing these issues will be presented in Section 4.

2.1 Issues with CE Loss

Even when a classifier produces outputs that do an excellent job of correctly classifying the input, the CE loss is far from zero with a substantial derivative towards higher confidence. This is illustrated in the first row of Table 1 which shows losses for example outputs produced by a 4-way classifier. On each presentation of a correctly classified example the non-zero CE loss will cause the outputs to become ever more extreme (highly positive for the logit representing the correct class and highly negative for the logits representing the incorrect classes). CE loss therefore encourages a DNN to map every training exemplar to an output where confidence is extremely high. It is to be expected that such a DNN will produce high confidence for all samples, including ones not seen during training. Hence, it is unsurprising that CE-trained DNNs have issues using prediction confidence to distinguish known from unknown classes.

Another issue that effects CE loss is shown in the remaining rows of table Table 1. Intuitively, the predictions get worse from top to bottom as the output of the first neuron (representing the true class of the sample) gets less distinct from the response of the other neurons as we go down the table. The output shown on the last row is clearly the worst, as the network predicts the wrong class label with high confidence. It should therefore be expected that the loss will increase from a minimum

Table 1: Example outputs (logits), \mathbf{y} , from the last layer of an imaginary neural network being trained to perform a 4-way classification task (*i.e.*, $n = 4$), and the corresponding losses associated with each of these predictions when the first output, y_1 , represents the correct class. Hyper-parameters for each loss were set to $\tau = 1$ for cross-entropy (CE) loss, $\tau = 0.04$ for LogitNorm (LN) loss, and $\mu = 0.5$ for multi-class margin (MM) and high error margin (HEM).

\mathbf{y}	CE	LN	MM	HEM
[1.0 -1.0 -1.0 -1.0]	0.34	0.00	0.00	0.00
[0.6 0.1 0.1 0.1]	1.04	0.00	0.00	0.00
[0.6 0.3 0.0 -0.1]	1.02	0.00	0.11	0.45
[0.6 0.5 0.0 -0.7]	1.00	0.09	0.16	0.63
[0.6 0.7 0.0 -3.5]	0.98	1.10	0.19	0.77
[0.0 1.0 0.0 0.0]	1.74	25.00	0.66	0.88

in the top row to a maximum in the bottom row. However, the behaviour of CE loss is inconsistent with this expectation. Essentially, CE loss can be reduced by making the difference in output between the true class and another already rejected class larger without increasing the difference to the closest competitor class. As a result, CE loss can be lower when the classifier incorrectly classifies the sample (penultimate row), compared to situations where the classifier succeeds in making the correct prediction (second to fourth rows).

The remaining columns of Table 1 show that LogitNorm (LN), and multi-class margin (MM), both described in Section 3, and the proposed loss, high error margin (HEM) that will be described in Section 4, do not suffer from either of these issues. These losses produces a loss of zero for samples where the output of the neuron representing the true class is sufficiently larger than the outputs of other neurons (top rows) and non-zero losses only for predictions that are worse at distinguishing the true class from the alternatives (bottom rows). In the case of MM and HEM, this is due to these losses using a margin. In the case of LN loss this behaviour is due to it behaving like a margin loss (Section 3.3).

Another issue with CE loss continuing to update the weights even when the task has been learnt successfully, is that this will cause weights to be over-written. We hypothesised that this might be one reason why learning with imbalanced training data is difficult: even once the classifier has learnt to correctly classify samples from the majority class, each presentation of such samples in future training epochs will result in weight changes that will make the model better able to map inputs to the class labels of the majority classes, but reduce the capacity of the model to represent mappings from minority samples to their class labels. This is consistent with findings that models learn fewer features relevant to the minority classes than the majority classes (Dablain et al., 2024).

The over-writing of weights is also an issue in continual learning. Even when classes in later learning episodes have been adequately learnt, CE loss will continue to update the weights, causing further forgetting of the tasks that were learnt earlier. In contrast, a margin-based loss will stop updating the weights once the model has learnt the new task, preserving more of the previously learnt information.

2.2 Issues with MM Loss

The above analysis suggests that a margin-based loss should have advantages over CE loss. However, MM loss produces classifiers that have significantly lower accuracy on the standard test data compared to equivalent CE-trained classifiers (as shown in Fig. 1). We put this down to the method used to combine the errors (see Section 3.6). Averaging the errors (across logits and samples in the batch) causes MM loss to become close to zero prior to all samples being correctly classified (especially when there are many classes). Hence, MM loss effectively terminates weight updates prematurely. The low loss is the result of averaging the errors when many of these values are zero at the later stages of learning. Summing the errors might alleviate this issue, but would result in very large losses early in training when there a many non-zero (and potentially large) errors. It would also result in the initial magnitude of the loss varying with the number of classes in the data-set. In either case (averaging or summing), the loss at the start of learning is much higher than the loss near the end of learning, and this tends to cause MM loss to fail to suppress the last non-zero errors during the later stages of training.

3 Existing Loss Functions

For each input image \mathbf{x} , a classifier, g , produces a vector of outputs, each element of which is associated with a class label, *i.e.*: $\mathbf{y} = g(\mathbf{x})$, where $\mathbf{y} \in \mathbb{R}^n$, and n is the number of classes. For a neural network these outputs are the activations of the neurons in the last layer before applying an activation function. These values are commonly known as the “logits” following a literal interpretation of the cross-entropy loss. The class label, c , predicted by such a classifier is that associated with the output with the highest value, *i.e.*, $c = \operatorname{argmax}(\mathbf{y})$.

In addition to predicting the class of the input sample, the classifier can also provide an estimate of its confidence in the classification it has made. Two standard methods of confidence scoring are Maximum Logit Score (MLS; Hendrycks et al., 2022a; Vaze et al., 2022), and Maximum Softmax Probability (MSP; Hendrycks and Gimpel, 2017). MLS is the maximum

response of the network output before any activation function is applied, *i.e.*, $\max(\mathbf{y})$. MSP is the maximum value of the network output after the application of the softmax activation function, *i.e.*, $\max(\mathbf{z})$ where \mathbf{z} is defined as:

$$z_j = \frac{\exp(\frac{y_j}{\tau})}{\sum_{i=1}^n \exp(\frac{y_i}{\tau})} \quad (1)$$

τ is a non-negative hyper-parameter that is typically set to a value of one. The softmax function normalises the output values so that they sum to one and can be interpreted as a probability distribution. Smaller values of τ cause the softmax function to produce a more peaked probability distribution.

The output of the network is also used to define a differentiable loss function that is used to update the parameters so that predictions become more accurate. Those existing loss functions most relevant to this work are described in the following sections.

3.1 Cross-Entropy Loss

Cross-Entropy (CE) loss is defined as:

$$\mathcal{L}_{CE} = -\log z_l \quad (2)$$

where l is the index corresponding to the correct class (*i.e.*, the ground-truth class label), and \mathbf{z} is the output of the softmax activation function applied to the logits (Eq. (1)). As described earlier, the softmax function has a hyper-parameter, τ , which means that CE could be applied using different values of this parameter. However, for almost all applications of CE, τ is set to a value of one. Hence, a value of $\tau = 1$ was used in all experiments with CE loss described in this paper.

3.2 LogitNorm Loss

LogitNorm (LN) loss is a variation of CE loss that has been shown to produce state-of-the-art results on unknown class rejection when used in conjunction with the Maximum Softmax Probability (MSP) confidence scoring method (Wei et al., 2022). LN loss makes two modifications to CE loss: (1) it normalises the logits by their l_2 -norm before application of the softmax function, (2) it uses a low value of τ that causes the softmax function to produce a more peaked probability distribution. Preliminary experiments (B.1) showed that a hyper-parameter of $\tau = 0.04$ was most effective at unknown class rejection, and hence, that value was used in all experiments with LN loss described in this paper.

3.3 LogitNorm Loss as a Margin-like Loss

The LogitNorm loss yields values close to zero when the output of the correct neuron is sufficiently larger than the other neurons' outputs (Table 1). This behaviour is due to the use of a reduced value of τ . When τ is sufficiently small the softmax function produces a highly peaked probability distribution and $\frac{\exp(\frac{y_l}{\tau})}{\sum_{i=1}^n \exp(\frac{y_i}{\tau})} \rightarrow 1$. This causes LN loss to be zero when the response of the node corresponding to the correct class is sufficiently dominant. Hence, LN loss behaves like a margin loss, as learning stops for samples that are sufficiently well classified. We believe this margin-like behaviour, which prevents increasing confidence, explains the effectiveness of LN loss at distinguishing known from unknown classes.

In contrast, Wei et al. (2022) claim that the effectiveness of LN loss is due to the normalisation of the logits. They believe that normalisation forces learning to generate logit vectors for different classes that are distinct from each other in terms of the angle between them, rather than their magnitude. While we do not believe that normalisation is the primary factor in avoiding over-confidence, normalisation provides other advantages. The normalisation of the logits is responsible for the loss monotonically increasing as the predictions become worse (this is true even when $\tau = 1$). Large negative logits produced by neurons that do not represent the true class (activities that would reduce CE loss) cause a reduction in the normalised logit value associated with the true class, and hence, increase the LN loss. The normalisation of the logits performed by LN also seems to be important to prevent training becoming unstable: we found that LN loss was capable of successfully training networks with small τ values, while the same small τ values would cause CE loss to fail. The cause of this instability is possibly that a low value of τ can result in the loss being very large when the prediction is very wrong (see last row of Table 1), a situation that is common early in training when the network's outputs are random.

3.4 Logit-adjusted Loss

Logit-adjusted (LA) loss is a variation of CE loss that is designed to produce improved performance when training with imbalanced data (Menon et al., 2021). Before the application of the softmax function, the logits are modified by a term that is proportional to the relative number of training samples in each class. Hence,

$$\mathcal{L}_{LA} = -\log z'_l \quad (3)$$

where:

$$z'_j = \frac{\exp(y_j + \log(p_j))}{\sum_{i=1}^n \exp(y_i + \log(p_i))} \quad (4)$$

The term p_j is the proportion of training samples in class j , i.e. $p_j = s_j / \sum_{i=1}^n s_i$ where s_j is the number of samples in class j . A number of similar losses have been proposed which use alternative methods to adjust the logits (Cao et al., 2019; Ren et al., 2020; Tan et al., 2020). However, LA loss has been found to produce better results than these alternatives and other methods of dealing with class imbalance (Menon et al., 2021; Zhao et al., 2024). Note, that for balanced data-sets, p_j has the same value for each class and LA loss is identical to CE loss.

3.5 DICE Loss

DICE loss (Milletari et al., 2016) is an alternative to CE that is frequently used for image segmentation tasks (Azad et al., 2023; Ma et al., 2021). It uses a measure of the overlap between the one-hot encoded target outputs, \mathbf{t} , and the softmax predictions, \mathbf{z} , such that:

$$\mathcal{L}_{DICE} = 1 - 2 \frac{\sum_i (t_i \times z_i)}{\sum_i (t_i + z_i)} \quad (5)$$

In multi-class applications, DICE loss is calculated separately for each class (the sums in Eq. (5) are taken over the samples in the batch), and the overall DICE loss is the mean of the separate class losses.

3.6 Multi-class Margin Loss

Multi-class Margin (MM) loss, also known as the classification hinge loss (Crammer and Singer, 2002), defines an error, e_i , associated with each logit, y_i , as follows:

$$e_i = \begin{cases} \max(0, y_i - y_l + \mu_i) & \text{if } i \neq l \\ 0 & \text{if } i = l \end{cases} \quad (6)$$

where $\mu_i = \mu \forall i$, and μ is the margin, a non-negative hyper-parameter. Note, that although MM loss employs the same margin for all outputs, we have specified per-logit margins in equation Eq. (6) as these will be exploited by the proposed loss (see Section 4.3). The error is zero for samples that produce an output from the neuron representing the correct class that is larger than μ above the output produced by any other output neuron. MM loss combines the error for different logits (and across all samples in a batch) by taking the mean, so that:

$$\mathcal{L}_{MM} = \frac{1}{n} \sum_{i=1}^n e_i \quad (7)$$

Preliminary experiments (B.1) showed that the value of the margin had little influence on classification accuracy, but had a stronger influence on unknown class rejection performance. A value of $\mu = 1$ was used in all subsequent experiments as this was most effective at unknown class rejection and is the default value typically used for this loss.

4 High Error Margin Loss

4.1 Combining Errors to Calculate HEM Loss

We hypothesised (Section 2) that the ineffectiveness of multi-class margin (MM) loss is a result of the way the errors (Eq. (6)) are combined. Our proposed loss function, HEM, therefore combines the errors in a different manner.

For each sample, all error values below the mean are set to zero, and the mean of above-zero values is calculated:

$$\mathcal{L}_{HEM} = \frac{\sum_{i=1}^n (\mathbb{1}[e_i \geq \frac{1}{n} \sum e_j] \times e_i)}{\sum_{i=1}^n \mathbb{1}[e_i \geq \frac{1}{n} \sum e_j]} \quad (8)$$

$\mathbb{1}[\cdot]$ is the indicator function, which equals 1 if the argument is true and 0 otherwise. Losses for different samples in the batch are also combined by finding the mean of above-zero values. Note that the computation of the mean error, used by the indicator function in Eq. (8), is detached from the computational graph so that it does not affect the gradients.

At the start of learning, when a large number of logits produce errors (especially when n is large), the mean error for each sample will be significant and by only considering those losses above the mean HEM concentrates on reducing the largest errors. Later in learning, there will be many zero errors and as a result, the mean error will be small (likely smaller than the few non-zero errors that remain). Hence, at this stage in training thresholding the errors by the mean will have little effect. However, by taking the mean of only the above-zero values, the loss will remain large even when there are few non-zero errors in each sample, and/or few incorrectly classified samples in a batch. As a result, HEM loss concentrates on the logits that produce the highest errors throughout learning.

The effectiveness of the proposed method of combining error, compared to that used in Multi-class margin (MM) loss, was confirmed in an ablation study presented in B.2.

4.2 Setting the Margin for HEM

HEM has one hyper-parameter: the margin, μ . Based on preliminary experiments (see B.1) it was decided to set the margin used in HEM loss to be equal to $\sqrt{M/\sum_{i=1}^n s_i}$, where s_i is the number of samples in class i and M was fixed at 2000. This method of setting the margin was used in all subsequent experiments with HEM.

4.3 High Error Margin with adjusted margins (HEM+)

HEM+ is a variation on HEM designed to help deal with class imbalance. For HEM+ we propose a second modification compared to MM loss. Specifically, separate margins for each logit, where the value of each margin is inversely proportional to the number of training samples associated with that class, *i.e.*, $\mu_i = \sqrt{M/(ns_i)}$. Note that when the training data contains the same number of samples per class all the margins are equal and HEM+ is identical to HEM.

5 Results

We compared the performance of networks trained with our proposed loss, HEM, to the performance of identical networks trained with the alternative losses described in Section 3. We have sought to produce a fair and representative evaluation of the different losses by using many different tasks, data-sets, and network architectures. Performance was tested using a number of different metrics to assess accuracy, generalisation, and robustness. Note that for all metrics larger values correspond to better performance.

The tasks were chosen to include essential and important applications in computer vision (image classification and semantic segmentation), and tasks where we expected our margin loss to perform well, due to it not learning to make predictions with very high confidence (unknown class rejection) and stopping weight updates once adequate performance is achieved (continual learning and learning with imbalanced data).

For all experimental conditions (combination of data-set, network architecture, and loss function) a network was trained and evaluated multiple times (usually 5 times), each time with a different random weight initialisation and random presentation order of training samples. The mean and standard-deviation over these trials is reported for each metric used. Each experiment was performed using a single NVIDIA Tesla V100 GPU with 16GB of memory, except for experiments with ImageNet1k which were executed in parallel on four such GPUs. Full details of the tasks, data-sets, evaluation metrics, DNN architectures and training set-ups are provided in A.

5.1 Learning with Standard Data-sets

Performance on image classification tasks was assessed using using five standard data-sets: MNIST, CIFAR10, CIFAR100, TinyImageNet and ImageNet1k using a total of 14 different neural network architectures ranging in size from LeNet (20,194 parameters) to Vit-B/16 (86,567,656 parameters). Performance was evaluated in terms of several criteria: ability to classify the standard test data, ability to generalise to corrupted test data, ability to identify and reject samples from unknown classes, and the ability to either correctly classify or reject adversarially perturbed samples. Full details of the experimental methods are provided in A.1.

5.1.1 Performance on standard test data and common corruptions data

Networks trained using CE loss and HEM loss have comparable performance on classifying the standard test data (Fig. 2(a)) and the common corruptions data (Fig. 2(b)), however, CE loss has a small, but consistent advantage. On average this advantage for clean accuracy is around $\approx 1\%$ across the fifteen conditions (five data-sets with three network architectures per data-set) that we have used, as shown in Fig. 2(c). This difference in average performance can also be seen in Fig. 1 which shows relative rather than absolute performance. Accuracy on clean and corrupt test data is similar for HEM and LN, while the performance of HEM far exceeds that of the other losses we have tested: DICE and MM.

Classification accuracy measured on the standard test set, which contains samples from a similar input distribution to the training data, has been the main pre-occupation of most research in the history of machine learning so far. On such data, as confirmed by our results, CE loss performs the best and for this reason has become the standard loss function for training classifiers. However, more recently, there has been growing concern that accuracy on the standard test data is insufficient to ensure DNN classifiers are safe, reliable, and trustworthy in more realistic scenarios (Akhtar and Mian, 2018; Amodei et al., 2016; Bowers et al., 2023; Geirhos et al., 2020, 2018; Heaven, 2019; Ilyas et al., 2019; Marcus, 2020; Nguyen et al., 2015; Papernot et al., 2016; Roy et al., 2022; Sa-Couto and Wichert, 2021; Serre, 2019; Spratling, 2023; Yuille and Liu, 2021).

5.1.2 Performance on unknown class rejection and AutoAttack rejection.

It is well known that CE-trained DNNs are susceptible to making over-confident predictions. For example, when shown samples that do not belong to any of classes in the training data a DNN may predict with high confidence that these samples belong to one of the known categories (Amodei et al., 2016; Hendrycks and Gimpel, 2017; Kumano et al., 2022; Nguyen et al., 2015). Such over-confidence for unknown classes has the potential to cause errors in real-world scenarios where such

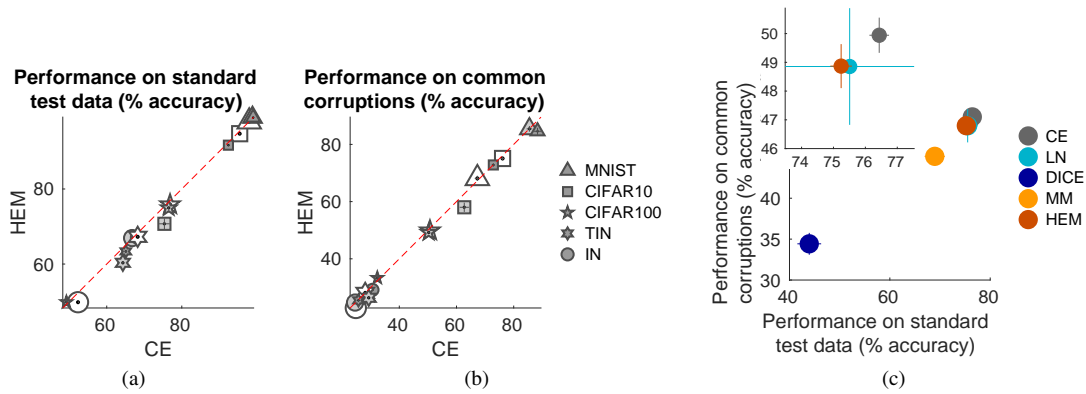


Figure 2: Results when learning with standard data-sets and testing with clean and corrupt images. (a) and (b) directly compare the performance produced by HEM and cross-entropy (CE) losses when used to train networks with MNIST, CIFAR10, CIFAR100, TinyImageNet (TIN), and ImageNet1k (IN) using three different network architectures for each data-set. For each data-set the size of the marker used corresponds to the size of the network. Results above the diagonal are conditions where better performance was obtained when training with HEM rather than CE loss. Performance metrics are averaged over multiple trials performed for each condition (data-set and architecture) and the error bars show the standard deviation recorded across the trials in each condition (in the majority of cases these error bars are too small to be visible). (a) Compares the performance of the two losses in terms of the accuracy of classifying the standard test-data. (b) Compares the performance of the two losses in terms of the accuracy of classifying the common-corruptions test-data. (c) Shows results averaged over all the data-sets and network architecture (and multiple trials in each condition) for all relevant losses: cross-entropy (CE), LogitNorm (LN), DICE, multi-class margin (MM) and HEM. Error bars show the mean standard deviation recorded across the trials in each condition. The inset shows the results for CE, LN, and HEM losses plotted on a separate scale to allow the differences between these losses to be visible.

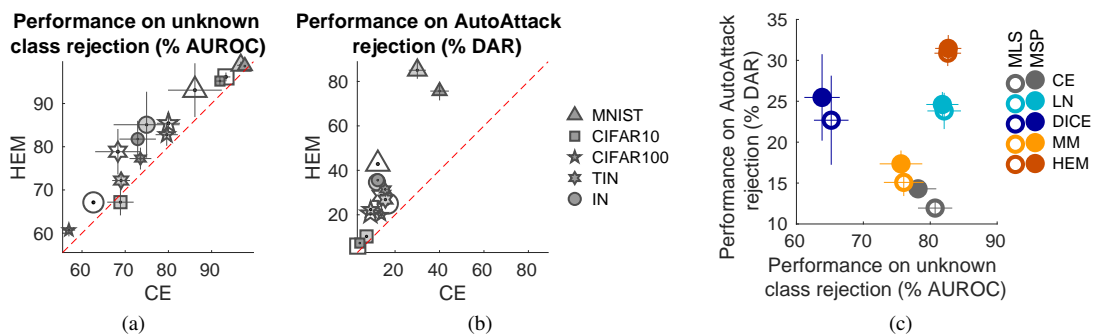


Figure 3: Results when learning with standard data-sets and testing on unknown and adversarial images. This figure has an identical format to Fig. 2 except (a) compares the performance of CE and HEM losses in terms of the ability to distinguish samples from known and unknown classes, and (b) compares the performance of CE and HEM losses in terms of the ability to deal correctly with adversarially perturbed samples. In both (a) and (b) Maximum Softmax Probability (MSP) is used as the confidence score. (c) Shows results averaged over all the data-sets and network architecture (and multiple trials in each condition) for all relevant losses. Closed markers indicate that Maximum Softmax Probability (MSP) was used as the confidence score, while open markers plot results when using Maximum Logit Score (MLS).

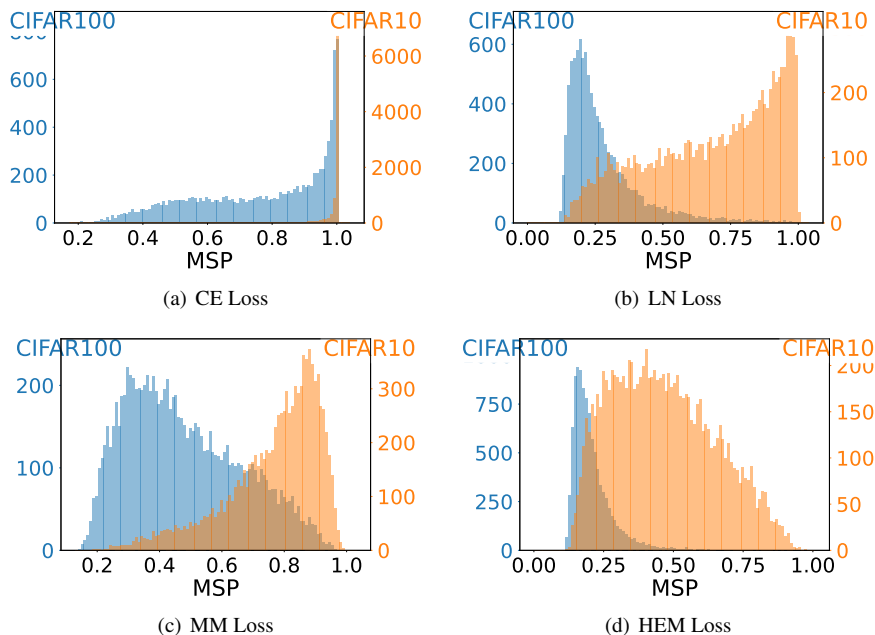


Figure 4: Prediction confidence after learning with standard data-sets. Results are for WRN22-10 networks trained on CIFAR10. Each graph shows histograms of the number of samples classified with different levels of prediction confidence (MSP). Separate histograms are shown for the response generated to unseen samples from known classes (the CIFAR10 test set) and unknown classes (the CIFAR100 test set). The former is measured against the right-hand vertical axis and the latter against the left-hand vertical axis.

samples might be commonly encountered and in situations where dishonest actors deliberately attempt to fool the classifier into making erroneous predictions.

To evaluate how susceptible a network is to this kind of overconfidence error, one can test whether it is more certain in its prediction for samples that belong to the classes used for training than for samples that do not belong into any of the training classes. Formally, one evaluates how well these two cases can be distinguished based on a confidence score. This evaluation method is called open-set recognition (Vaze et al., 2022; Yang et al., 2022), out-of-distribution (OOD) detection/rejection (Bitterwolf et al., 2022; Hendrycks and Gimpel, 2017; Hendrycks et al., 2022b; Mohseni et al., 2020; Zhang and Ranganath, 2023), or unknown class rejection (Spratling, 2023). Our results demonstrate that CE-trained networks have significantly worse performance than those trained using the proposed loss (Fig. 3(a)). In all but one of the fifteen conditions we tested HEM outperforms CE. HEM-trained networks have a similar, large and consistent, advantage over identical CE-trained architectures in terms of detecting adversarial attacks (Fig. 3(b)). Compared to CE, HEM loss has a much larger advantage in terms of its ability to enable accurate unknown class rejection, and also to detect adversarial attacks, than the small disadvantage it has in terms of clean and corrupt accuracy.

On average across the fifteen conditions (five data-sets with three network architectures per data-set) that we have used, HEM is the best performing loss on these tasks (Fig. 3(c) and Fig. 1 for the same averaged results in terms of relative rather than absolute performance). HEM loss trains classifiers that are better able to distinguish unknown and adversarial images even than LN trained networks, even though LN is a specialised loss that produces state-of-the-art performance on unknown class rejection.

As expected given the analysis in Section 2, CE loss tends to produce very high confidence for most samples (Fig. 4(a)). In contrast, the margin-like losses produce a much wider range of prediction confidence values for the known data (Figs. 4(b) to 4(d)). This was expected as none of these losses can be optimised by increasing the magnitude of the logits vector, and hence, the MSP. This confirms that the advantages in unknown class rejection we observe for LN and HEM losses are indeed due to less severe overconfidence. MM loss fails to improve unknown class rejection performance beyond that of CE loss, and typically results in lower accuracy on the standard test data, particularly for data-sets with a large number of classes. As discussed in Section 2, an explanation for these empirical observations is that the MM loss tends to become close to zero prior to all samples being correctly classified (especially when n is large), and hence, MM loss effectively terminates weight updates prematurely.

5.2 Learning with Imbalanced Data-sets

The ability to learn when the training data contained a very different number of samples for different classes (*i.e.*, with long-tailed data) was tested using the CIFAR10 and CIFAR100 training data. This training data was modified, using the standard methods using in the previous literature to produce long-tailed data by removing different numbers of samples from each

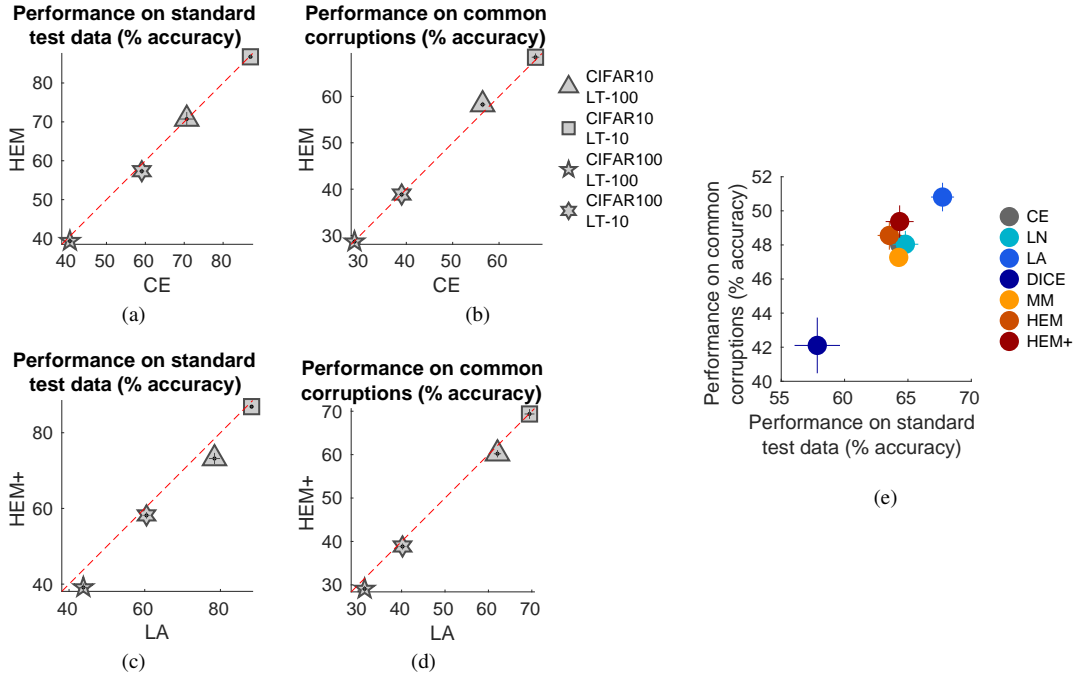


Figure 5: Results when learning with imbalanced data-sets and testing on clean and corrupt images. (a) and (b) directly compare the performance produced by HEM and cross-entropy (CE) losses when used to train networks with long-tailed (LT) CIFAR10 and CIFAR100 each with imbalance factors 100 and 10. ResNet32 was used for the CIFAR10 data and ResNet18 for the CIFAR100 data. (c) and (d) show the same comparisons for HEM+ and LA losses. (e) Shows results averaged over all the data-sets and network architectures (and five trials in each condition) for all relevant losses: cross-entropy (CE), LogitNorm (LN), logit-adjusted (LA), DICE, multi-class margin (MM), HEM, and HEM+ losses. The format of this figure is otherwise the same as, and described in the caption of, Fig. 2.

class. Performance was evaluated on two network architectures using all the performance criteria used in the previous section to evaluate networks trained with balanced data-sets. Full details of the experimental methods are provided in A.2.

A comparison of the performance of networks trained on imbalanced data using CE and HEM losses reveals similar pattern of results as where obtained with standard training data. Specifically, similar performance for the two losses on standard (Fig. 5(a)) and corrupt (Fig. 5(b)) test data, better performance with HEM loss for unknown class rejection (Fig. 6(a)) and adversarial sample rejection (Fig. 6(b)).

Comparing LA and HEM+ losses (*i.e.*, versions of CE and HEM modified to improve performance on imbalanced data) shows that LA has an advantage in terms of clean (Fig. 5(c)) and corrupt (Fig. 5(d)) accuracy, but that HEM-trained networks are better at identifying, and rejecting, unknown (Fig. 6(c)) and adversarial samples (Fig. 6(d)). The high performance of LA loss on the clean data raises the prospect that there may be more optimal settings for the margins in HEM+. Future work might usefully explore alternative heuristics for setting the margins or ways of learning margins for different tasks.

Results averaged over the four conditions (and 5 trials per condition) for these four losses, plus LN, DICE and MM show that LN performs similarly to HEM (or HEM+) on three of the four evaluation metrics, but produces worse results on adversarial attacks. DICE loss performs significantly worse than HEM (or HEM+) on all evaluation criteria, except for rejection of adversarial samples, where DICE loss (using the Maximum Logits Score) is superior. These averaged results can be seen in in Figs. 5(e) and 6(e). Fig. 1 also includes the same averaged results, in terms of relative rather than absolute performance.

5.3 Continual Learning

The performance of HEM loss when applied to continual learning was assessed using standard benchmark tasks: Permut-edMNIST, SplitMNIST, SplitCIFAR10, and SplitCIFAR100. Due to catastrophic forgetting (French, 2003), the over-writing of previously learned weights when training on a new task, all loss functions perform very poorly at continual learning unless a strategy is used to reduce forgetting. Many such strategies have been proposed. Here five were used: Replay (Chaudhry et al., 2019; Robins, 1993), Synaptic Intelligence (SI; Zenke et al., 2017), Elastic Weight Consolidation (EWC; Kirkpatrick et al., 2017), Less-Forgetful Learning (LFL; Jung et al., 2016), and Learning without Forgetting (LwF; Li and Hoiem, 2016). Each loss function was used in combination with these continual learning strategies, and performance was evaluated at the end of a sequence of five training episodes using unseen test data for all the five sub-tasks that were learnt during training. Full details of the experimental methods are provided in A.3

Our proposed loss performed better at continual learning than CE loss consistent with our expectations (Section 2).

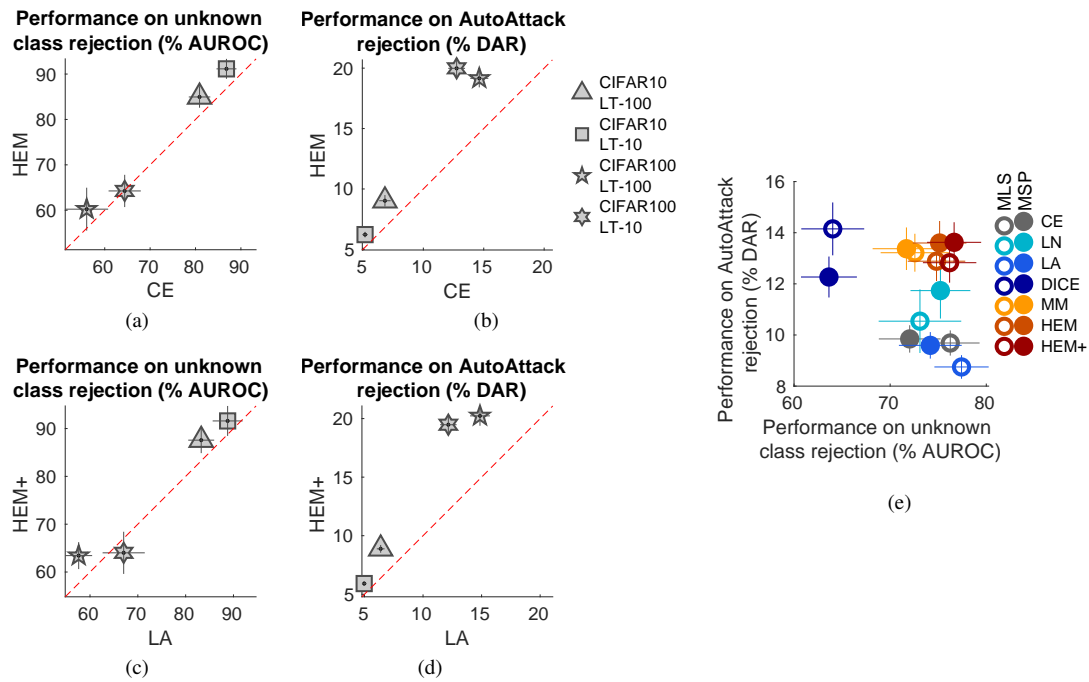


Figure 6: Results when learning with imbalanced data-sets and testing on unknown and adversarial images. This figure has an identical format to Fig. 5 except (a) and (c) compares performance of pairs of losses in terms of the ability to distinguish samples from known and unknown classes, and (b) and (d) compares the performance of pairs of losses in terms of the ability to deal correctly with adversarially perturbed samples. In (a) to (d) Maximum Softmax Probability (MSP) is used as the confidence score. (e) Shows results averaged over all the data-sets and network architecture (and five trials in each condition) for all relevant losses. Closed markers indicate that Maximum Softmax Probability (MSP) was used as the confidence score, while open markers plot results when using Maximum Logit Score (MLS). The format of this figure is otherwise the same as, and described in the caption of, Fig. 3.

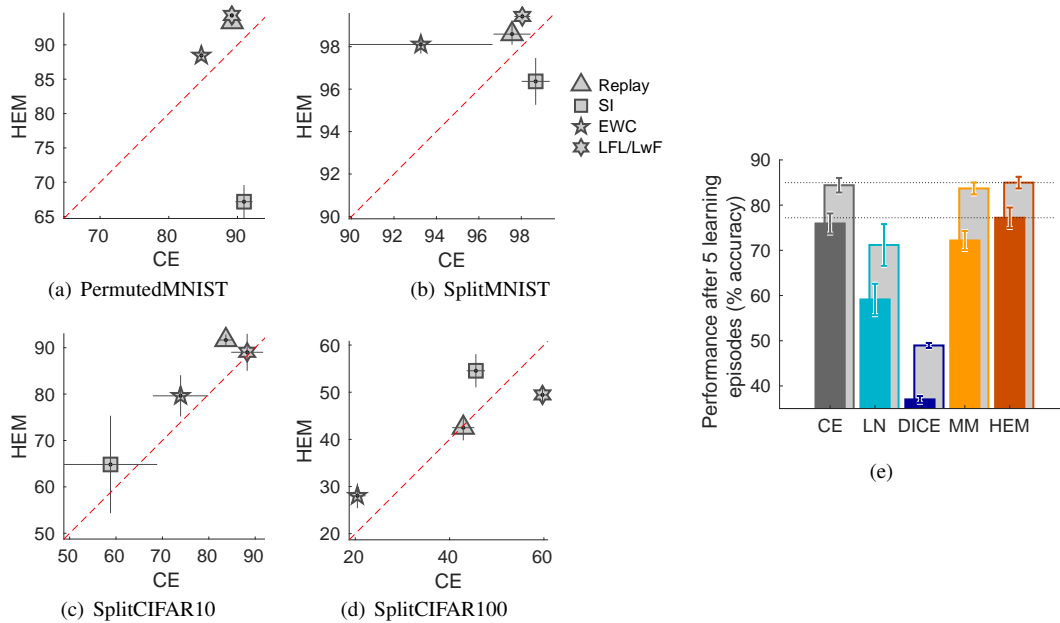


Figure 7: Results for continual learning. (a) to (d) directly compare the performance produced by HEM and cross-entropy (CE) losses when applied to the PermutedMNIST, SplitMNIST, SplitCIFAR10 and SplitCIFAR100 tasks. Results above the diagonal are conditions where better performance was obtained when training with HEM rather than CE loss. Performance is measured as accuracy on the test data for all tasks after training on a sequence of five tasks. Error bars show the standard deviation recorded over five trials. Experiments were performed using a number of techniques to reduce the effects of catastrophic forgetting: Replay, Synaptic Intelligence (SI), Elastic Weight Consolidation (EWC), Less-Forgetful Learning (LFL), and Learning without Forgetting (LwF). LFL was used for PermutedMIST and LwF for the other tasks. (e) Shows results averaged over the four tasks and the four methods of reducing catastrophic forgetting applied to each task (and five trials in each condition) for all relevant losses: cross-entropy (CE), LogitNorm (LN), DICE, multi-class margin (MM), and HEM. Error bars show the mean standard deviation recorded across five trials in each condition. The light grey bars show results averaged over task and trials when for each loss only the best performing method of reducing catastrophic forgetting is chosen.

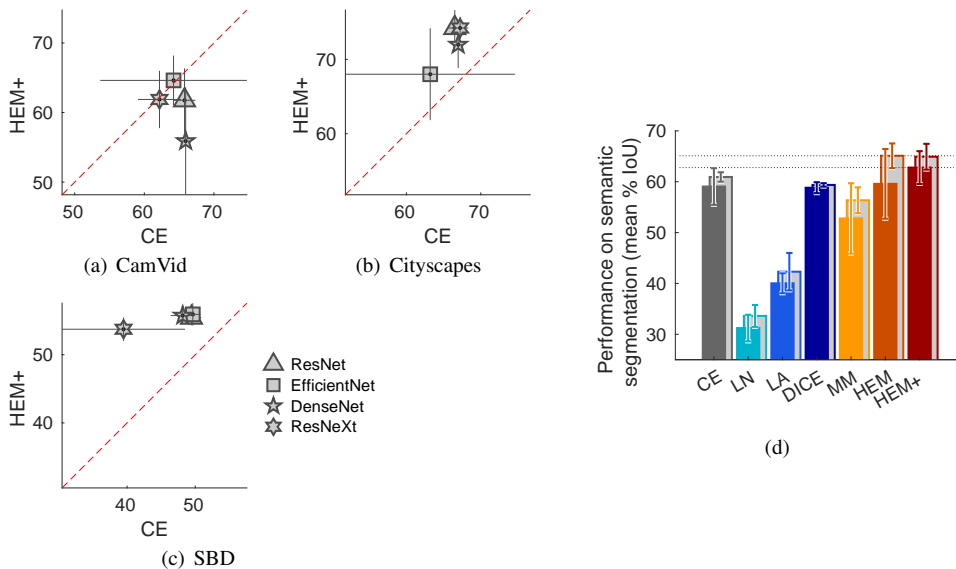


Figure 8: Results for semantic segmentation. (a), (b), and (c) directly compare the performance produced by HEM+ and cross-entropy (CE) losses when applied to the CamVid, Cityscapes, and SBD benchmarks. Results above the diagonal are conditions where better performance was obtained when training with HEM+ rather than CE loss. Performance is measured as mean percentage Intersection-over-Union (IoU). Results are averaged over five trials performed for each encoder-backbone architecture (ResNet34, EfficientNet-b4, DenseNet201, and ResNeXt50). Error bars show the standard deviation recorded over the five trials for each condition. (d) Shows results averaged over the three data-sets and four encoder-backbone architectures (and five trials in each condition) for all relevant losses: cross-entropy (CE), LogitNorm (LN), Logit-adjusted (LA), DICE, multi-class margin (MM), HEM, and HEM+. Error bars show the mean standard deviation recorded across five trials in each condition. The light grey bars show results averaged over data-set and trials when for each loss only the backbone architecture that produces the best results is chosen.

Specifically, in 11 of the 16 conditions tested, considerably better performance was obtained using HEM loss rather than CE loss (Figs. 7(a) to 7(d)). Furthermore, if only the best performing combination of loss and strategy of reducing catastrophic forgetting is considered for each loss, then in three of the four tasks HEM loss produces better performance than CE loss. This is remarkable as the training recipes used were designed to produce the best performance for each method of reducing catastrophic forgetting when paired with CE loss.

The advantage of HEM over CE is also evident when the results are averaged over conditions (and 5 trials per condition) as shown in Fig. 7(e) (relative performance is shown in Fig. 1). This data shows that HEM has even greater advantages over the other applicable losses that were tested: LN, DICE and MM. LN and DICE losses perform very poorly on continual learning. This suggests that, unlike HEM and CE losses, they do not generalise to tasks outside of the specialised domain for which they were developed. Note that as there is no class imbalance in the training data used here, LA and HEM+ are not considered (the results for these methods would be identical to those for CE and HEM respectively).

5.4 Semantic Segmentation

Performance on semantic segmentation was assessed using three standard data-sets: CamVid (Brostow et al., 2009), Cityscapes (Cordts et al., 2016), and SBD (Hariharan et al., 2011). For each data-set multiple experiments were performed using the FPN architecture (Kirillov et al., 2019) with four different backbones. Full details can be found in A.4.

For semantic segmentation, HEM+ shows considerably better average performance than CE, and all other losses considered (Fig. 8(d), relative performance is shown in Fig. 1). For some backbone architectures CE loss produced superior image segmentation performance to HEM+ loss on the CamVid data-set (Fig. 8(a)). However, for both of the larger data-sets, HEM+ loss out-performed CE loss with all four backbone architectures (Figs. 8(b) and 8(c)).

LN and LA losses perform very poorly (Fig. 8(d) and Fig. 1) showing that these specialised losses do not work outside of the specific domain for which they were created. DICE, another specialised loss, but one developed specifically for segmentation tasks has performance similar to that of CE loss and HEM loss. When the margins of our proposed loss are adjusted for class imbalance (HEM+) performance is superior to that produced by all the alternative losses. The advantage of HEM+ is even clearer if for each data-set only the results for the backbone architecture that gives the best results for each loss is considered (as shown by the light grey bars in Fig. 8(d)).

6 Conclusion

High error margin (HEM) loss trains substantially more robust DNNs than cross-entropy (CE) loss. The only tasks where CE loss performs slightly better is clean and corrupt image classification. In contrast, HEM loss far exceeds the performance of CE loss on rejecting out-of-distribution samples from unknown classes and adversarial samples. With imbalanced training data, HEM loss equals or exceeds the performance of CE loss in all metrics. For continual learning HEM loss works better than CE. For semantic segmentation HEM loss works as well as CE. Adjusting the margin based on the number of samples (HEM+), further improved performance for imbalanced data and semantic segmentation. As HEM+ is the same as HEM for balanced data, there are no conditions in which HEM+ had worse performance than HEM. Hence, HEM+ is a general-purpose loss that almost always performs better than CE loss. Following current standard practice we have separately assessed performance against different benchmarks. However, it is not hard to imagine real-world scenarios where multiple advantages of our loss might combine to yield even greater advantages over CE loss. For example, a task where it is necessary to learn continuously and the resulting classifier needs to be robust to unknown classes.

Specialised losses performed better than cross-entropy loss for the tasks they were designed for, but all failed on other tasks. In contrast, HEM and HEM+ losses performed well on all tasks. LogitNorm (LN) loss (Wei et al., 2022), performs almost as well as HEM loss at out-of-distribution rejection, but HEM out-performs LN by a considerable margin on continual learning and semantic segmentation. With imbalanced training data, logit-adjusted (LA) loss (Menon et al., 2021) yields better performance on standard test data than HEM+ loss, but HEM+ is superior at rejecting out-of-distribution samples. Furthermore, HEM+ out-performs LA at semantic segmentation, our only other task with class imbalance. For semantic segmentation the commonly used specialised loss, DICE (Milletari et al., 2016), performed no better than cross-entropy loss in the experimental set-ups we used. Hence, HEM+ loss performed semantic segmentation more accurately than DICE, and out-performed DICE by a considerable margin on all other tasks.

In all our experiments, our newly proposed loss was at a disadvantage because all training and evaluation choices were optimized for cross-entropy loss. This applies to the training hyper-parameters, the network architectures, the OOD rejection methods, and the continual learning techniques. Despite these disadvantages HEM trains classifiers that outperform those trained with CE loss, or are as good as those trained using CE loss, in all the tasks we have considered except clean image classification with balanced training data. However, this difference is negligible, as optimising the training hyper-parameters can yield much bigger improvements in clean accuracy than the difference we observe (He et al., 2018; Pang et al., 2021; Wightman et al., 2021). A simple experiment where only the initial learning rate was modified based on intuition gained from observing the learning dynamics substantiates this claim (see B.3).

Replacing cross-entropy loss with HEM+ loss seems worthwhile under almost all circumstances. Replacing the loss function is a simple modification that comes at no additional development or computational cost. HEM+ loss generally performs well across a wide range of dataset sizes, tasks and network architectures that we tested. We tested only image classification here, but do not see any reason why HEM+ loss should not work for other classification tasks.

Acknowledgements

The authors gratefully acknowledge use of the King’s Computational Research, Engineering and Technology Environment (CREATE) and the HPC facilities of the University of Luxembourg (Varrette et al., 2022) for carrying out the experiments described in this paper.

A Experimental Methods

A.1 Learning with Standard Data-sets

A.1.1 Training Data

Performance was assessed for DNNs trained on standard image classification data-sets: MNIST, CIFAR10, CIFAR100, TinyImageNet (TIN) and ImageNet1k (IN). These data-set vary in terms of the size of the images (from 28-by-28 pixels with 1 colour channel to 224-by-224 pixels with 3 colour channels), the number of categories (10 to 1000), and the number of training samples (from 50k to 1.28M). For all datasets, standard data augmentations were applied to the training images: horizontal flipping and random cropping for both CIFAR data-sets and TinyImageNet, horizontal flipping, resizing to 256 pixels, and a centre crop for ImageNet1k. For all data-sets the standard split between training and testing exemplars was employed. Pixel values in both the training and testing samples were scaled to the range $[0,1]$.

A.1.2 Performance Metrics

Performance was evaluated against a number of different criteria.

Performance on standard test data Firstly, the percentage of samples correctly classified from the standard test set provided with each training data-set was calculated (the “clean” accuracy).

Performance on common corruptions data Secondly, the ability of trained networks to generalise to input distribution shifts was assessed by determining classification accuracy with the common corruptions data-sets: MNIST-C, CIFAR10-C, CIFAR100-C, TinyImageNet-C and ImageNet-C (Hendrycks and Dietterich, 2019; Mu and Gilmer, 2019). MNIST-C contains 15 different corruptions including different types of noise, blurring, geometric transformations, and superimposed patterns. The others contain 18 different corruptions including different types of noise, blurring, synthetic weather conditions, and digital corruptions. As is typical in the literature, performance was evaluated by averaging performance over all the corruptions at all degrees of intensity.

Performance on unknown class rejection A third performance metric was used to assess the ability of a network to distinguish known from unknown classes. This was evaluated using the Area Under the Receiver Operating Characteristic curve (AUROC) as this is a common choice in the literature (Chen et al., 2023; Cheng et al., 2023; Kirchheim et al., 2022; Lee et al., 2022; Xu-Darme et al., 2023; Yang et al., 2022, 2023). AUROC is calculated separately for each unknown class data-set, evaluating how distinct the confidence scores produced by samples from the standard test-set are from the confidence scores produced in response to samples from the unknown class data-set. The standard, baseline, method for determining confidence uses the maximum value of the network output after the application of the softmax activation function (*i.e.*, $\max(\mathbf{z})$). As a result it is called Maximum Softmax Probability (MSP; Hendrycks and Gimpel, 2017). MSP was used by default in our assessment, but some evaluations were repeated using an alternative: Maximum Logit Score (MLS; Hendrycks et al., 2022a; Vaze et al., 2022). MLS defines the confidence that a sample is of a known class as the maximum response of the network output before any activation function is applied (*i.e.*, $\max(\mathbf{y})$).

AUROC was calculated using seven data-sets containing unknown classes, and the average AUROC across all seven data-sets was reported. The seven data-set used to evaluate networks trained with MNIST were the test-sets of Omniglot (Lake et al., 2015), FashionMNIST (Xiao et al., 2017), KMNIST (Clanuwat et al., 2018) and four data-sets containing synthetic images: (1) images containing random blobs, as used in (Hendrycks et al., 2019); (2) images in which each pixel intensity value was independently and randomly selected from a uniform distribution; (3) the images of the standard (clean) test set after a random permutation of all pixels; (4) the images of the clean test set after randomising the phase, in the Fourier domain, of each image. Each of these four synthetic data-sets contained 10000 samples. The CIFAR10 trained networks were tested using unknown classes from the test-sets of the Textures (Cimpoi et al., 2014), SVHN (Netzer et al., 2011), and CIFAR100 data-sets, plus, four synthetic image data-sets generated as described before. For CIFAR100 trained networks the same seven OOD data-sets were used as for CIFAR10, except CIFAR10 was used in place of CIFAR100. Networks trained on TinyImageNet and ImageNet1k were evaluated using Textures (Cimpoi et al., 2014), the iNaturalist 2021 validation set (Van Horn et al., 2018), the ImageNet-O data-set (Hendrycks et al., 2021), and the four synthetic image data-sets generated as described previously.

Performance on AutoAttack rejection Finally, performance was also evaluated using adversarial attacks generated using AutoAttack (AA; Croce and Hein, 2020), a state-of-the-art ensemble attack method that employs both gradient-based (white-box) and gradient-free (black-box) attacks. AA was implemented using the torchattacks PyTorch library (Kim, 2021). Two sets of adversarial samples were created. Each set was created by perturbing 10000 samples from the standard (clean) test-set, but with a different method of constraining the magnitude of the perturbation. Specifically, AA was used to apply both l_∞ and l_2 -norm constrained attacks. The perturbation budget (ϵ) used for each attack was the standard value used in the previous literature for each data-set. Specifically, ϵ was set to $\frac{8}{255}$ and 0.5 for l_∞ and l_2 -norm attacks, respectively, against

Table 2: A summary of the neural network architectures used to assess performance on image classification when learning with standard data-sets. For each model the number of trainable parameters is indicated in brackets. For each data-set the architectures are arranged from left-to-right in order of increasing size. Note that ResNet50 and ResNet18 are large networks designed for use with ImageNet1k (but using a different stem when applied to smaller images), while ResNet32 is a smaller network designed for use with CIFAR10, and hence, has fewer parameters than ResNet18 despite its greater depth.

Data-set	Model 1	Model 2	Model 3
MNIST	LeNet (20,194)	ConvNet (30,954)	MLP (239,410)
CIFAR10	ResNet32 (464,154)	MobileNetS (1,528,106)	WRN22-10 (27,977,146)
CIFAR100	MobileNetL (4,330,132)	ResNet18 (11,173,962)	PARN18 (11,218,340)
TinyImageNet	ResNet18 (11,173,962)	inception (23,995,504)	WRN28-10 (38,241,656)
ImageNet1k	ResNet50 (25,557,032)	SwinT (28,351,570)	ViT-B/16 (86,567,656)

networks trained on CIFAR10, CIFAR100, TinyImageNet, and ImageNet1k, and ϵ was set to 0.3 for l_∞ -norm and to 2 for l_2 -norm attacks on MNIST trained networks.

Networks were not trained to be able to correctly classify adversarial examples, and hence, robust accuracy was low for all the evaluated losses. However, networks can still be robust if they are capable of identifying, and rejecting samples that have been adversarially perturbed. Adversarial robustness was evaluated using detection accuracy rate (DAR; [Spratling, 2023](#)). DAR determines the proportion of samples that are processed correctly. Where for adversarial samples, “processed correctly” means that the sample is accepted and the predicted class label is correct, or it is rejected and the predicted class label is wrong ([Zhu et al., 2024](#)). As for unknown class rejection, a sample is accepted or rejected based on the confidence of the prediction made by the network under evaluation. Confidence was measured using either Maximum Softmax Probability (MSP) or Maximum Logit Score (MLS), and the threshold used to reject samples was set such that 95% of correctly classified samples from the standard test set were accepted ([Zhu et al., 2024](#)).

A.1.3 Neural Network Architectures

A large variety of DNNs architectures were used as summarised in Table 2. A small version of LeNet ([LeCun et al., 1998](#)) with 16 channels in the two convolutional layers, and 50 neurons in the penultimate, fully-connected, layer. A simple, fully-convolutional neural network (ConvNet) consisting of 5 convolutional layers, each containing 32 3-by-3 masks and using the ReLU activation function. This architecture performed down-sampling using average pooling and it did not use batch (or any other form of) normalisation. It is a simple, sequential, hierarchy without any parallel pathways or skip connections. A simple fully-connected network (MLP) consisting of three hidden layers each containing 200 neurons and employing the ReLU activation function. ResNets ([He et al., 2016a](#)), specifically, ResNet18, ResNet32, and ResNet50. WideResNets ([Zagoruyko and Komodakis, 2016](#)), specifically, WRN22-10 and WRN28-10. PreActResNet18 (PARN18; [He et al., 2016b](#)). MobileNet version 3 ([Howard et al., 2019, 2017](#)), specifically the small model (MobileNetS) and the large model (MobileNetL). The inception architecture version 3 ([Szegedy et al., 2015, 2016](#)). The Swin Transformer (version 2) ([Liu et al., 2022, 2021](#)) tiny (SwinT). The vision transformer ([Dosovitskiy et al., 2020](#)) base model with 16×16 input patch size (ViT-B/16).

Our implementations of ResNets, WRNs, and PARN were based on the code provided with ([Pang et al., 2021](#)),^a except for the implementation of ResNet32 which was adapted from code by Yerlan Idelbayev,^b and ResNet50 which came from the PyTorch Hub.^c The implementations of MobileNet3, inception3, and the Transformers were also from the PyTorch Hub. The inception3 was modified to allow it to work with TinyImageNet as follows. Before the inception layers the original architecture, designed for use with the larger images in ImageNet1k, contains three standard convolution layers, a max pooling layer, two further standard convolution layers, and another max pooling layer. Both maxpooling and the two convolution layers between them were removed. Furthermore, the size of the filters in the second convolutional layer in the auxiliary head were changed from 5-by-5 to 4-by-4.

A.1.4 Training Settings

To ensure a fair comparison between loss functions, while avoiding the need to search for optimal training hyper-parameters for each combination of loss function, network architecture and data-set, the same training hyper-parameters were used for all the experiments performed using the same combination of data-set and network architecture. In general, five repeats were made of each experiment, except those experiments performed with ImageNet1k where either three repeats (when using the two smaller models listed in Table 2) or one experiment (using the largest model listed in Table 2) were performed.

MNIST For all experiments with MNIST, training was performed for 20 epochs using the Adam optimiser ([Kingma and Ba, 2015](#)) with a batch size of 128 and a fixed learning rate of 10^{-3} . This set-up was found in preliminary experiments to be adequate for obtaining high test-set accuracy when training ConvNet with CE loss.

^a<https://github.com/P2333/Bag-of-Tricks-for-AT>

^bhttps://github.com/akamaster/pytorch_resnet_cifar10/

^c<https://pytorch.org/vision/stable/models.html>

CIFAR10 and CIFAR100 For training with both CIFAR data-sets, the SGD optimiser was used for 110 epochs with a momentum of 0.9, a batch size of 128, weight decay of $5e-4$, an initial learning rate of 0.1 and a step-wise learning schedule reducing the learning rate by a factor of 10 at epochs 100 and 105. This set-up was taken from (Pang et al., 2021) where it was found to be optimal for the adversarial-training of networks using CE loss. As we are not using adversarial training, this set-up is probably sub-optimal for all the loss functions we compare. If it does favour one loss function, that is likely to be CE. Using this training setup with MobileNets resulted in poor results: CIFAR100 clean accuracy of less than 50% with all loss functions, and chance accuracy on one trial with LN loss. A search for a better initial learning rate (with all other learning hyper-parameters as described before), performed using CE loss and CIFAR100, found that a value of 0.02 produced the best performance. This lower initial learning rate was therefore used for all experiments with MobileNet.

TinyImageNet For training networks on TinyImageNet more epochs are required to reach reasonable performance. Hence, compared to the settings for CIFAR, the number of epochs was increased to 200. Furthermore, the training schedule was changed to decay (by a factor of 10) the learning rate at 50, 100, and 150 epochs. Except for an additional learning rate decay at 50 epochs, the resulting set-up is identical to that used in (Rice et al., 2020), for adversarially-training networks with CE loss.

ImageNet1k With the ImageNet1k data-set the ResNet50 architecture was trained using SGD for 100 epochs with a momentum of 0.9, a batch size of 512, weight decay of $1e-4$, and an initial learning rate of 0.1 that decayed by a factor of 10 at epochs 25, 50, and 75. This recipe uses a larger batch size, 10 more epochs, and one more learning rate decay, but is otherwise the same as baseline training method typically used for training ResNet50 on ImageNet1k.^d For training the Swin Transformer on ImageNet1k the set-up was based on that proposed in Irandoust et al. (2022). Namely, using the AdamW optimiser with a fixed learning rate of 10^{-3} preceded by an exponential learning-rate warm-up period of five epochs.^e Training was performed for 100 epochs with a batch size of 256. This same set-up, but with a 10 epoch warm-up period, was used to train the ViT-B/16 architecture.

A.2 Learning with Imbalanced Data-sets

A.2.1 Training Data

Learning with imbalanced training data was assessed using long-tailed versions of CIFAR10 and CIFAR100. These are standard benchmark tasks in this domain, where the training data is generated from the original, balanced, data-sets by removing samples unequally from each class. Specifically, each long-tailed data-set is created by taking only the first $s_j \times f^j$ samples for the class with index j ($j \in \{0, \dots, n-1\}$). f is a factor that determines the degree of imbalance. From CIFAR100 two long-tailed data-sets were created using $f = 0.6$ and $f = 0.7744$, and from CIFAR10 two long-tailed data-sets were created using $f = 0.955$ and $f = 0.9771$. The first value of f for each data-set generates a long-tailed set in which the ratio of the number of samples in the classes with the largest and smallest numbers is 100. The second values of f produce an imbalance ratio of 10.

A.2.2 Performance Metrics

Performance was assessed using standard, balanced, test-data sets. The same range of evaluation metrics were used as were used to assess the performance of networks trained on standard training data-sets (as described in A.1.2).

A.2.3 Neural Network Architectures

ResNet32 was trained on the long-tailed CIFAR10 data-sets, and ResNet18 was used for the long-tailed CIFAR100 data-sets.

A.2.4 Training Settings

The training set-up was based on that used in previous work with the same training data (Cao et al., 2019; Cui et al., 2019). Specifically, networks were trained for 200 epochs using SGD with a momentum of 0.9, a batch size of 128, weight decay of $2e-4$, and an initial learning rate of 0.1, that was reduced by a factor of 100 at the end of epochs 160 and 180.

A.3 Continual Learning

A.3.1 Training Data

Performance on continual learning was assessed with the aid of the Avalanche library (Carta et al., 2023; Lomonaco et al., 2021) using four standard benchmark tasks: PermutedMNIST, SplitMNIST, SplitCIFAR10, and SplitCIFAR100. In each case models were trained on a sequence of five sub-sets of data (training “episodes”). Each trial used a different, randomly

^d<https://pytorch.org/blog/how-to-train-state-of-the-art-models-using-torchvision-latest-primitives/>

^eThe warm-up period was extended to 10 epochs when using CE loss, as training with the original set-up resulted in a training collapse and final training set accuracy at chance level.

selected, sequence of training data sub-sets, and this same sequence of sub-tasks was used with each loss to ensure a fair comparison. Each loss function was tested in combination with five strategies for reducing catastrophic forgetting: Replay (Chaudhry et al., 2019; Robins, 1993), Synaptic Intelligence (SI; Zenke et al., 2017), Elastic Weight Consolidation (EWC; Kirkpatrick et al., 2017), Less-Forgetful Learning (LFL; Jung et al., 2016), and Learning without Forgetting (LwF; Li and Hoiem, 2016). The tasks and continual learning strategies were chosen as code for implementing them was available in the Continual Learning Baselines repository.^f

A.3.2 Performance Metrics

Performance was evaluated at the end of training by measuring classification accuracy with an unseen test set containing equal numbers of samples from each sub-task.

A.3.3 Neural Network Architectures

For each combination of task and continual learning strategy we used the same neural network architecture as used in the Continual Learning Baselines repository. For the MNIST tasks the networks were MLPs, while for the CIFAR tasks the architecture was a ResNet18.

A.3.4 Training Settings

For each combination of task and continual learning strategy we used the same training set-up as used in the Continual Learning Baselines repository. Where this repository only provided a training recipe for MNIST (or CIFAR10/100), we altered it for use with the other data-sets only by changing the number of epochs (so that the number was 10 times larger for the CIFAR data-sets than for MNIST).

A.4 Semantic Segmentation

A.4.1 Training Data

Performance on semantic segmentation was assessed with the aid of the Pytorch Segmentation Models Library^g using three data-sets: CamVid (Brostow et al., 2009), Cityscapes (Cordts et al., 2016), and SBD (Hariharan et al., 2011).

A.4.2 Performance Metrics

In each case, performance was evaluated using the mean percentage intersection-over-union (IoU) metric.

A.4.3 Neural Network Architectures

All experiments were performed with the FPN architecture (Kirillov et al., 2019) using four different networks as the encoder-backbone: ResNet34 (He et al., 2016a), EfficientNet-b4 (Tan and Le, 2019), DenseNet201 (Huang et al., 2017), and ResNeXt50 (Xie et al., 2017).

A.4.4 Training Settings

The training set-up was based on that used previously for training on the CamVid data-set (Badrinarayanan et al., 2017). Specifically, SGD with momentum of 0.9 was used with a fixed learning rate of 0.1 and a batch size of 12. As not all data-sets contain separate test and validation data a fixed number of training epochs was used, rather than selecting the best checkpoint as was done by Badrinarayanan et al. (2017). 100 epochs was used for CamVid and 50 epochs were used for the other two, larger, data-sets. For the larger data-sets we reduced the batch size to four in order to fit within GPU memory.

For the SBD data-set, CE loss failed to learn when using a learning rate of 0.1. A hyper-parameter search was therefore carried out using CE loss to test alternative learning rates (0.05, 0.02, 0.005, 0.001). A learning rate of 0.05 was found to work best with CE loss, so this learning rate was used in all experiments with all losses and the SBD data-set.

A.5 Code

Open-source code implemented using Python using the PyTorch library (Paszke et al., 2019) is available from: <https://codeberg.org/mwspratling/HEMLoss/>.

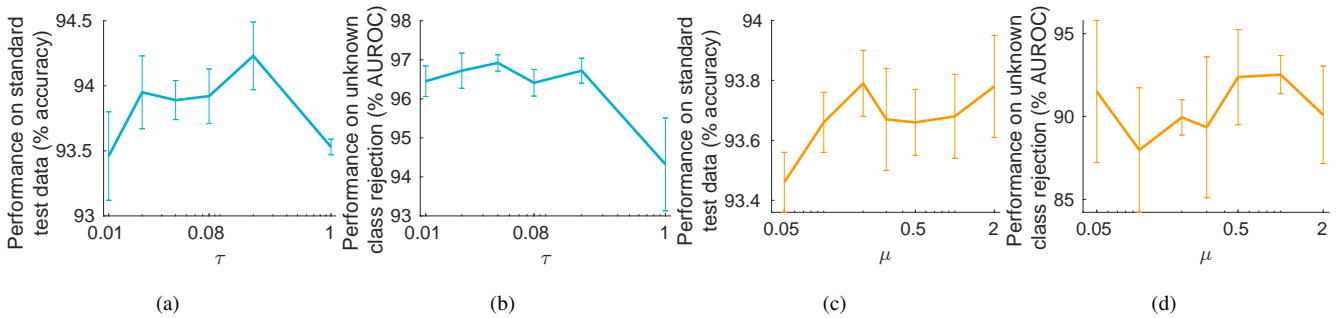


Figure 9: The effects of the loss hyper-parameter on LogitNorm (LN) and Multi-class Margin (MM) losses. Results for LN are shown in (a) and (b). Results for MM are shown in (c) and (d). Performance metrics are averaged over five trials performed with each parameter value, and the error bars show the standard deviation recorded across these five trials. Experiments were performed using the ResNet18 architecture trained using the standard training data for CIFAR10. Performance was evaluated using accuracy on the standard (clean) test data-set (a) and (c), and using AUROC to evaluate the accuracy with which known and unknown classes can be distinguished when Maximum Softmax Probability is used as the confidence score (b) and (d).

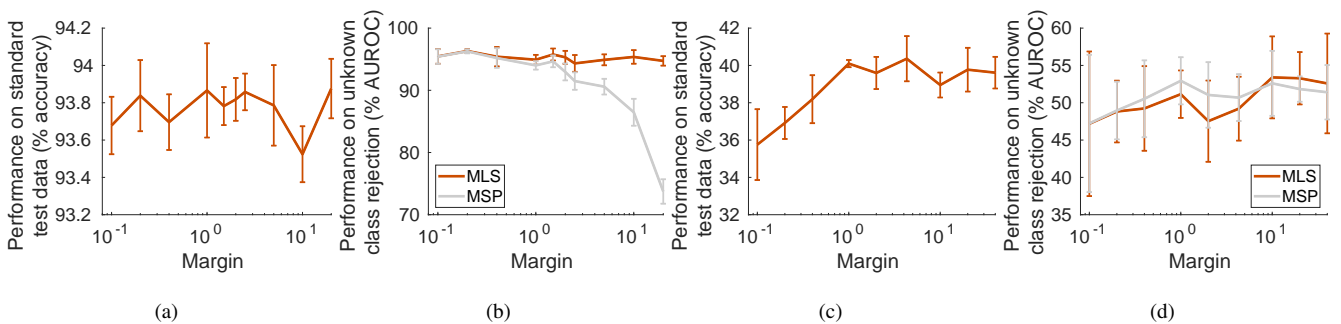


Figure 10: The effects of the HEM loss margin. Performance metrics are averaged over five trials performed with each margin value, and the error bars show the standard deviation recorded across these five trials. Experiments were performed using the ResNet18 architecture. Results in (a) and (b) are for networks trained using the full CIFAR10 training dataset. Results in (c) and (d) are for networks trained using a reduced CIFAR10 training dataset containing 50 samples per class. (a) and (c) show the effect of the margin on the accuracy of classifying the CIFAR10 test-set. (b) and (d) show the effects of the margin on the ability to identify, and reject, samples from unknown classes. Performance is averaged over seven out-of-distribution data-sets and the rejection criteria is based on either Maximum Softmax Probability (MSP) or Maximum Logit Score (MLS).

B Supplementary Experiments

B.1 Loss Hyper-parameter Selection

One of the great advantages of CE loss is that it does not introduce additional hyper-parameters that need to be tuned for different network architectures and tasks. Ideally, an alternative loss should also work without the need for hyper-parameter tuning. Preliminary experiments were performed to select an appropriate value for the hyper-parameter of each loss function that introduces such a parameter. These experiments were carried out using ResNet18 networks trained on CIFAR10: a combination of network architecture and data-set that was not used in the main experiments. The training set-up was as described in A.1 for training other ResNets, WRNs and PARN on CIFAR data. Results for these preliminary experiments are shown in Fig. 9 for LN and MM losses, and Fig. 10 for HEM loss.

For HEM, we expected that the results would be insensitive to the choice of μ as learning would scale the magnitude of the logits to match the chosen margin. Consistent with this expectation, the accuracy in classifying the CIFAR10 test set was fairly constant for networks trained using margin values ranging over more than two orders of magnitude (Fig. 10(a)). The choice of margin does, however, effect the ability to differentiate known and unknown classes using the Maximum Softmax Probability (MSP) confidence score, as shown in Fig. 10(b). A large margin will cause the network to learn to produce high magnitude logits. The softmax function applied to larger magnitude logits will produce a more peaked distribution. As a result, the confidence in the prediction being made when measured using MSP, for both known and unknown classes, will be higher and it will become more difficult to distinguish known from unknown classes. However, even with a large margin, it

^f<https://github.com/ContinualAI/continual-learning-baselines>

^ghttps://github.com/qubvel/segmentation_models.pytorch

Table 3: Ablation study on the effects of the proposed changes to MM loss on classification accuracy. Results are for ResNet18 networks trained on CIFAR10 and CIFAR100 using a margin of $\mu = 0.2$. Results are averaged over five trials and the standard deviation is given after the \pm symbol. The best result in each column is highlighted in bold. The changes made to standard MM loss are denoted as “maz” for taking the mean of above-zero errors, and “thres” for setting errors below the mean to zero.

Loss	Clean Accuracy (%)	
	CIFAR10	CIFAR100
MM	93.79 \pm 0.11	70.13 \pm 0.19
+maz	93.81 \pm 0.23	74.94 \pm 0.35
+thres	93.78 \pm 0.22	73.13 \pm 0.26
+maz+thres = HEM	93.84\pm 0.19	74.95\pm 0.46

is possible perform unknown class rejection if Maximum Logit Score (MLS) is used as the measure of prediction confidence (Fig. 10(b)).

If the the margin is reduced so that it approaches zero (or becomes negative) performance should degrade, as the classifier will not have learnt to produce higher logits for the correct class. For example, ResNet18 networks trained on CIFAR10 with HEM loss and $\mu = 0$ have mean standard test-set accuracy of 90.7% (*cf.*, with the results in Fig. 10(a)). We expected that the point at which the performance would degrade would depend on the number of training exemplars. When there are few training exemplars a larger margin is likely to be required in order allow accurate generalisation, whereas, when there are many training exemplars the decision boundary can be positioned more accurately and a smaller margin is sufficient to separate samples from different classes. To demonstrate this the previous experiments were repeated using a version of the CIFAR10 training data-set that contained only 50 samples per class (rather than the 5000 samples per class in the full CIFAR10 training set). As can be seen from Fig. 10(c), a larger margin is required to reach the upper limit of accuracy in this case. Based on these results it was decided to set the margin used in HEM loss to be equal to $\sqrt{M/\sum_{i=1}^n s_i}$, where s_i is the number of samples in class i and M was fixed at 2000. This equates to $\mu = 0.2$ for the full CIFAR10 training set, and $\mu = 2$ for the 50 samples per class version.

B.2 Ablation Study

The proposed loss, HEM, is a variation on MM loss. The effects of the proposed modifications were tested using ResNet18 networks trained on CIFAR10 and CIFAR100. The training set-up was as described in Appendix A.1.

The first modification is to include only above-zero error values when calculating the mean error. It can be seen from Table 3 that this modification alone produces an improvement in classification accuracy. As expected, this improvement is greatest for the data-set with the most class labels, as there will be more zero-valued errors across the larger number of logits that this modification enables the loss to ignore.

The second modification made to MM loss was to set errors less than the mean to zero. On its own this modification is less effective than the first. This is to be expected, as this modification causes even more zeros to be included in the average, causing the loss to become low and learning to prematurely cease. However, when this modification is combined with the first it provides a small additional boost to performance by encouraging the loss to concentrate on the largest errors, particularly at the start of training when there are many errors. The advantage of HEM over MM in terms of clean accuracy is fairly small for the conditions shown in Table 3. However, as shown in Fig. 2(c), on average, over many data-sets and network architectures, the advantages of HEM over MM are significant.

B.3 Analysis of Learning

To check that our loss leads to equally effective learning as CE loss we investigated the changes in various metrics over the course of training (see Fig. 11). A major difference between CE and HEM loss is that the latter does not monotonically reduce over the whole course of training. This is to be expected, as only errors greater than the average contribute to the loss. Hence, it is possible that parameter updates during learning cause errors to move from just above the average to below the average. This will increase the mean of the remaining errors. Hence, it is important to prevent the calculation of the average from being used in the calculation of the gradients.

It can be seen that HEM benefits most from the drop in learning rate near the end of training and that there are large fluctuations in the loss, and the other recorded metrics, before the learning rate drop at 100 epochs. Both these observations suggest that HEM might benefit from a lower initial learning rate. This was confirmed experimentally by reducing the initial learning rate from 0.1 to 0.05. This increased performance for WRN22-10 networks trained on CIFAR10 with HEM loss on all the metrics used in this paper: the mean clean accuracy increased from 94.73% to 95.32%, the mean accuracy on common corruption increased from 75.08% to 75.41%, the mean AUROC for unknown class rejection increased from 96.16% to 96.56%, and mean DAR for adversarial attacks increased from 5.91% to 6.34%. Further improvements in performance might be expected by more carefully tuning the learning hyper-parameters for each task.

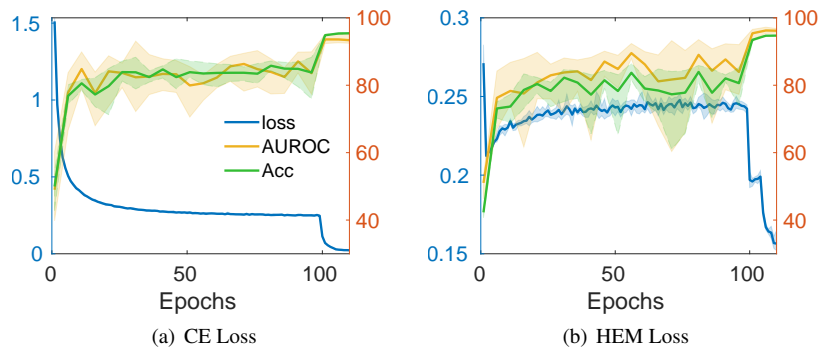


Figure 11: Learning dynamics for WRN22-10 networks trained on CIFAR10 with (a) cross-entropy (CE) loss, (b) high error margin (HEM) loss. Each graph shows the change during training of the loss, the mean percentage AUROC averaged over seven data-sets containing unknown classes (see A.1.2), and the percentage clean accuracy on the standard test-set. The loss is measured against the left-hand vertical axis and the others two metrics against the right-hand axis. The solid lines show the mean values over five trials, and the shaded regions indicate the minimum and maximum values recorded in any of the five trials.

HEM loss is zero for any training sample where the activation of the target logit is sufficiently above the value of the other logits. This means that during the later stages of learning many training samples cause no changes to the network weights. Future work might explore if this property could be exploited to reduce training time by avoiding repeatedly presenting to the network training samples that have been learnt. Alternatively, future work might explore if such training samples could be augmented to improve generalisation, or if regularisation terms could be added to HEM loss to improve the representations that are learnt.

References

- Akhtar, N. and Mian, A. (2018). Threat of adversarial attacks on deep learning in computer vision: A survey. *IEEE Access*, 6:14410–30. doi:[10.1109/ACCESS.2018.2807385](https://doi.org/10.1109/ACCESS.2018.2807385).
- Amodei, D., Olah, C., Steinhardt, J., Christiano, P., Schulman, J., and Mané, D. (2016). Concrete problems in AI safety. [arXiv:1606.06565](https://arxiv.org/abs/1606.06565).
- Awasthi, P., Mao, A., Mohri, M., and Zhong, Y. (2023). Theoretically grounded loss functions and algorithms for adversarial robustness. In Ruiz, F., Dy, J., and van de Meent, J.-W., editors, *Proceedings of the International Conference on Artificial Intelligence and Statistics (AISTATS)*, volume 206 of *Proceedings of Machine Learning Research*, pages 10077–94. <http://proceedings.mlr.press/v206/awasthi23c.html>.
- Azad, R., Heidary, M., Yilmaz, K., Hüttemann, M., Karimijafarbigloo, S., Wu, Y., Schmeink, A., and Merhof, D. (2023). Loss functions in the era of semantic segmentation: A survey and outlook. [arXiv:2312.05391](https://arxiv.org/abs/2312.05391).
- Badrinarayanan, V., Kendall, A., and Cipolla, R. (2017). Segnet: A deep convolutional encoder-decoder architecture for image segmentation. doi:[10.1109/TPAMI.2016.2644615](https://doi.org/10.1109/TPAMI.2016.2644615).
- Bitterwolf, J., Meinke, A., Augustin, M., and Hein, M. (2022). Breaking down out-of-distribution detection: Many methods based on OOD training data estimate a combination of the same core quantities. In *Proceedings of the International Conference on Machine Learning*, volume 162 of *Proceedings of Machine Learning Research*, pages 2041–74. [arXiv:2206.09880](https://arxiv.org/abs/2206.09880).
- Bowers, J. S., Malhotra, G., Dujmović, M., Montero, M. L., Tsvetkov, C., Biscione, V., Puebla, G., Adolphi, F., Hummel, J. E., Heaton, R. F., Evans, B. D., Mitchell, J., , and Blything, R. (2023). Deep problems with neural network models of human vision. *Behavioral and Brain Sciences*, in press. doi:[10.1017/S0140525X22002813](https://doi.org/10.1017/S0140525X22002813).
- Brostow, G. J., Fauqueur, J., and Cipolla, R. (2009). Semantic object classes in video: A high-definition ground truth database. *Pattern Recognition Letters*, 30(2):88–97. doi:[10.1016/j.patrec.2008.04.005](https://doi.org/10.1016/j.patrec.2008.04.005).
- Cao, K., Wei, C., Gaidon, A., Arechiga, N., and Ma, T. (2019). Learning imbalanced datasets with label-distribution-aware margin loss. In *Proceedings of the Conference on Advances in Neural Information Processing Systems*, pages 1567–78, Red Hook, NY, USA. Curran Associates Inc. [arXiv:1906.07413](https://arxiv.org/abs/1906.07413).
- Carta, A., Pellegrini, L., Cossu, A., Hemati, H., and Lomonaco, V. (2023). Avalanche: A pytorch library for deep continual learning. *Journal of Machine Learning Research*, 24(363):1–6. <http://jmlr.org/papers/v24/23-0130.html>.
- Chaudhry, A., Rohrbach, M., Elhoseiny, M., Ajanthan, T., Dokania, P. K., Torr, P. H. S., and Ranzato, M. (2019). On tiny episodic memories in continual learning. [arXiv:1902.10486](https://arxiv.org/abs/1902.10486).
- Chen, Y., Lin, Y., Xu, R., and Vela, P. A. (2023). WDiscOOD: Out-of-distribution detection via whitened linear discriminant analysis. In *Proceedings of the International Conference on Computer Vision*. [arXiv:2303.07543](https://arxiv.org/abs/2303.07543).
- Cheng, Z., Zhu, F., Zhang, X.-Y., and Liu, C.-L. (2023). Average of pruning: Improving performance and stability of out-of-distribution detection. [arXiv:2303.01201](https://arxiv.org/abs/2303.01201).
- Cimpoi, M., Maji, S., Kokkinos, I., Mohamed, S., , and Vedaldi, A. (2014). Describing textures in the wild. In *Proceedings of the IEEE Computer Society Conference on Computer Vision and Pattern Recognition*.
- Clanuwat, T., Bober-Irizar, M., Kitamoto, A., Lamb, A., Yamamoto, K., and Ha, D. (2018). Deep learning for classical japanese literature. In *Proceedings of the Conference on Advances in Neural Information Processing Systems*, Workshop on Machine Learning for Creativity and Design. [arXiv:1812.01718](https://arxiv.org/abs/1812.01718).
- Cordts, M., Omran, M., Ramos, S., Rehfeld, T., Enzweiler, M., Benenson, R., Franke, U., Roth, S., and Schiele, B. (2016). The cityscapes dataset for semantic urban scene understanding. In *Proceedings of the IEEE Computer Society Conference on Computer Vision and Pattern Recognition*. [arXiv:1604.01685](https://arxiv.org/abs/1604.01685).
- Crammer, K. and Singer, Y. (2002). On the algorithmic implementation of multiclass kernel-based vector machines. *Journal of Machine Learning Research*, 2:265–92.
- Croce, F. and Hein, M. (2020). Reliable evaluation of adversarial robustness with an ensemble of diverse parameter-free attacks. In *Proceedings of the International Conference on Machine Learning*, volume 119 of *Proceedings of Machine Learning Research*, pages 2206–16. [arXiv:2003.01690](https://arxiv.org/abs/2003.01690).
- Cui, J., Tian, Z., Zhong, Z., Qi, X., Yu, B., and Zhang, H. (2024). Decoupled kullback-leibler divergence loss. In *Proceedings of the Conference on Advances in Neural Information Processing Systems*. [arXiv:2305.13948](https://arxiv.org/abs/2305.13948).
- Cui, Y., Jia, M., Lin, T.-Y., Song, Y., and Belongie, S. (2019). Class-balanced loss based on effective number of samples. [arXiv:1901.05555](https://arxiv.org/abs/1901.05555).
- Dablain, D., Jacobson, K. N., Bellinger, C., Roberts, M., and Chawla, N. V. (2024). Understanding CNN fragility when learning with imbalanced data. *Machine Learning*, 113:4785–810. doi:[10.1007/s10994-023-06326-9](https://doi.org/10.1007/s10994-023-06326-9).
- Dosovitskiy, A., Beyer, L., Kolesnikov, A., Weissenborn, D., Zhai, X., Unterthiner, T., Dehghani, M., Minderer, M., Heigold, G., Gelly, S., Uszkoreit, J., and Houlsby, N. (2020). An image is worth 16x16 words: Transformers for image recognition at scale. In *Proceedings of the International Conference on Learning Representations*. [arXiv:2010.11929](https://arxiv.org/abs/2010.11929).
- French, R. M. (2003). Catastrophic forgetting in connectionist networks. In Nadel, L., editor, *Encyclopedia of Cognitive Science*, volume 1, pages 431–5. Nature Publishing Group, London, UK.
- Geirhos, R., Jacobsen, J.-H., Michaelis, C., Zemel, R., Brendel, W., Bethge, M., and Wichmann, F. A. (2020). Shortcut learning in deep neural networks. *Nature Machine Intelligence*, 2(11):665–73. doi:[10.1038/s42256-020-00257-z](https://doi.org/10.1038/s42256-020-00257-z). [arXiv:2004.07780](https://arxiv.org/abs/2004.07780).
- Geirhos, R., Temme, C. R. M., Rauber, J., Schütt, H. H., Bethge, M., and Wichmann, F. A. (2018). Generalisation in humans and deep neural networks. In *Proceedings of the Conference on Advances in Neural Information Processing Systems*.

[arXiv:1808.08750](https://arxiv.org/abs/1808.08750).

- Hariharan, B., Arbeláez, P., Bourdev, L., Maji, S., and Malik, J. (2011). Semantic contours from inverse detectors. In *Proceedings of the International Conference on Computer Vision*.
- He, K., Zhang, X., Ren, S., and Sun, J. (2016a). Deep residual learning for image recognition. In *Proceedings of the IEEE Computer Society Conference on Computer Vision and Pattern Recognition*, pages 770–8. [arXiv:1512.03385](https://arxiv.org/abs/1512.03385).
- He, K., Zhang, X., Ren, S., and Sun, J. (2016b). Identity mappings in deep residual networks. In *Proceedings of the European Conference on Computer Vision*. [arXiv:1603.05027](https://arxiv.org/abs/1603.05027).
- He, T., Zhang, Z., Zhang, H., Zhang, Z., Xie, J., and Li, M. (2018). Bag of tricks for image classification with convolutional neural networks. [arXiv:1812.01187](https://arxiv.org/abs/1812.01187).
- Heaven, D. (2019). Why deep-learning AIs are so easy to fool. *Nature*, 574:163–6.
- Hendrycks, D., Basart, S., Mazeika, M., Zou, A., Kwon, J., Mostajabi, M., Steinhardt, J., , and Song, D. (2022a). Scaling out-of-distribution detection for real-world settings. In *Proceedings of the International Conference on Machine Learning*. [arXiv:1911.11132](https://arxiv.org/abs/1911.11132).
- Hendrycks, D. and Dietterich, T. G. (2019). Benchmarking neural network robustness to common corruptions and perturbations. In *Proceedings of the International Conference on Learning Representations*. [arXiv:1903.12261](https://arxiv.org/abs/1903.12261).
- Hendrycks, D. and Gimpel, K. (2017). A baseline for detecting misclassified and out-of-distribution examples in neural networks. In *Proceedings of the International Conference on Learning Representations*. [arXiv:1610.02136](https://arxiv.org/abs/1610.02136).
- Hendrycks, D., Mazeika, M., and Dietterich, T. (2019). Deep anomaly detection with outlier exposure. In *Proceedings of the International Conference on Learning Representations*. [arXiv:1812.04606](https://arxiv.org/abs/1812.04606).
- Hendrycks, D., Zhao, K., Basart, S., Steinhardt, J., and Song, D. (2021). Natural adversarial examples. In *Proceedings of the IEEE Computer Society Conference on Computer Vision and Pattern Recognition*. [arXiv:1907.07174](https://arxiv.org/abs/1907.07174).
- Hendrycks, D., Zou, A., Mazeika, M., Tang, L., Li, B., Song, D., and Steinhardt, J. (2022b). Pixmix: Dreamlike pictures comprehensively improve safety measures. In *Proceedings of the IEEE Computer Society Conference on Computer Vision and Pattern Recognition*. [arXiv:2112.05135](https://arxiv.org/abs/2112.05135).
- Howard, A., Sandler, M., Chu, G., Chen, L., Chen, B., Tan, M., Wang, W., Zhu, Y., Pang, R., Vasudevan, V., Le, Q. V., and Adam, H. (2019). Searching for mobilenetV3. In *Proceedings of the International Conference on Computer Vision*. [arXiv:1905.02244](https://arxiv.org/abs/1905.02244).
- Howard, A. G., Zhu, M., Chen, B., Kalenichenko, D., Wang, W., Weyand, T., Andreetto, M., and Adam, H. (2017). Mobilenets: Efficient convolutional neural networks for mobile vision applications. [arXiv:1704.04861](https://arxiv.org/abs/1704.04861).
- Huang, G., Liu, Z., van der Maaten, L., and Weinberger, K. Q. (2017). Densely connected convolutional networks. In *Proceedings of the IEEE Computer Society Conference on Computer Vision and Pattern Recognition*. [arXiv:1608.06993](https://arxiv.org/abs/1608.06993).
- Ilyas, A., Santurkar, S., Tsipras, D., Engstrom, L., Tran, B., and Madry, A. (2019). Adversarial examples are not bugs, they are features. In Wallach, H., Larochelle, H., Beygelzimer, A., d’Alché-Buc, F., Fox, E., and Garnett, R., editors, *Proceedings of the Conference on Advances in Neural Information Processing Systems*, volume 32. Curran Associates, Inc. [arXiv:1905.02175](https://arxiv.org/abs/1905.02175).
- Irandoust, S., Durand, T., Rakhmangulova, Y., Zi, W., and Hajimirsadeghi, H. (2022). Training a vision transformer from scratch in less than 24 hours with 1 GPU. In *Proceedings of the Conference on Advances in Neural Information Processing Systems, Has it Trained Yet? Workshop*. [arXiv:2211.05187](https://arxiv.org/abs/2211.05187).
- Jung, H., Ju, J., Jung, M., and Kim, J. (2016). Less-forgetting learning in deep neural networks. [arXiv:1607.00122](https://arxiv.org/abs/1607.00122).
- Kanai, S., Yamaguchi, S., Yamada, M., Takahashi, H., Ohno, K., and Ida, Y. (2023). One-vs-the-rest loss to focus on important samples in adversarial training. In *Proceedings of the International Conference on Machine Learning*, volume 202 of *Proceedings of Machine Learning Research*. [arXiv:2207.10283](https://arxiv.org/abs/2207.10283).
- Kannan, H., Kurakin, A., and Goodfellow, I. (2018). Adversarial logit pairing. [arXiv:1803.06373](https://arxiv.org/abs/1803.06373).
- Kim, H. (2021). Torchattacks: a pytorch repository for adversarial attacks. [arXiv:2010.01950](https://arxiv.org/abs/2010.01950).
- Kingma, D. P. and Ba, J. (2015). Adam: A method for stochastic optimization. In *Proceedings of the International Conference on Learning Representations*. [arXiv:1412.6980](https://arxiv.org/abs/1412.6980).
- Kirchheim, K., Filax, M., and Ortmeier, F. (2022). Pytorch-OOD: A library for out-of-distribution detection based on pytorch. In *Proceedings of the IEEE Computer Society Conference on Computer Vision and Pattern Recognition, Workshops*, pages 4351–60. doi:[10.1109/CVPRW56347.2022.00481](https://doi.org/10.1109/CVPRW56347.2022.00481).
- Kirillov, A., Girshick, R., He, K., and Dollár, P. (2019). Panoptic feature pyramid networks. In *Proceedings of the IEEE Computer Society Conference on Computer Vision and Pattern Recognition*. [arXiv:1901.02446](https://arxiv.org/abs/1901.02446).
- Kirkpatrick, J., Pascanu, R., Rabinowitz, N., Veness, J., Desjardins, G., Rusu, A. A., Milan, K., Quan, J., Ramalho, T., Grabska-Barwinska, A., Hassabis, D., Clopath, C., Kumaran, D., and Hadsell, R. (2017). Overcoming catastrophic forgetting in neural networks. *Proceedings of the National Academy of Sciences USA*, 114(13):3521–6. doi:[10.1073/pnas.1611835114](https://doi.org/10.1073/pnas.1611835114).
- Kumano, S., Kera, H., and Yamasaki, T. (2022). Are DNNs fooled by extremely unrecognizable images? [arXiv:2012.03843](https://arxiv.org/abs/2012.03843).
- Lake, B. M., Salakhutdinov, R., and Tenenbaum, J. B. (2015). Human-level concept learning through probabilistic program induction. *Science*, 350(6266):1332–8. doi:[10.1126/science.aab3050](https://doi.org/10.1126/science.aab3050).
- LeCun, Y., Bottou, L., Bengio, Y., and Haffner, P. (1998). Gradient-based learning applied to document recognition. *Proceedings of the IEEE*, 86(11):2278–324. doi:[10.1109/5.726791](https://doi.org/10.1109/5.726791).
- Lee, J., Prabhushankar, M., and AlRegib, G. (2022). Gradient-based adversarial and out-of-distribution detection. In *Proceedings of the International Conference on Machine Learning, Workshop on New Frontiers in Adversarial Machine Learning*.

[arXiv:2206.08255](https://arxiv.org/abs/2206.08255).

- Li, Z. and Hoiem, D. (2016). Learning without forgetting. In *Proceedings of the European Conference on Computer Vision*, pages 614–29. [arXiv:1606.09282](https://arxiv.org/abs/1606.09282).
- Liu, Z., Hu, H., Lin, Y., Yao, Z., Xie, Z., Wei, Y., Ning, J., Cao, Y., Zhang, Z., Dong, L., Wei, F., and Guo, B. (2022). Swin transformer V2: Scaling up capacity and resolution. In *Proceedings of the IEEE Computer Society Conference on Computer Vision and Pattern Recognition*.
- Liu, Z., Lin, Y., Cao, Y., Hu, H., Wei, Y., Zhang, Z., Lin, S., and Guo, B. (2021). Swin transformer: Hierarchical vision transformer using shifted windows. In *Proceedings of the International Conference on Computer Vision*, pages 10012–22. [arXiv:2103.14030](https://arxiv.org/abs/2103.14030).
- Lomonaco, V., Pellegrini, L., Cossu, A., Carta, A., Graffieti, G., Hayes, T. L., Lange, M. D., Masana, M., Pomponi, J., van de Ven, G., Mundt, M., She, Q., Cooper, K., Forest, J., Belouadah, E., Calderara, S., Parisi, G. I., Cuzzolin, F., Tolia, A., Scardapane, S., Antiga, L., Amhad, S., Popescu, A., Kanan, C., van de Weijer, J., Tuytelaars, T., Bacciu, D., and Maltoni, D. (2021). Avalanche: an end-to-end library for continual learning. In *Proceedings of the IEEE Computer Society Conference on Computer Vision and Pattern Recognition*, 2nd Continual Learning in Computer Vision Workshop. [arXiv:2104.00405](https://arxiv.org/abs/2104.00405).
- Ma, J., Chen, J., Ng, M., Huang, R., Li, Y., Li, C., Yang, X., and Martel, A. L. (2021). Loss odyssey in medical image segmentation. *Medical Image Analysis*, 71:102035. doi:[10.1016/j.media.2021.102035](https://doi.org/10.1016/j.media.2021.102035).
- Mao, C., Zhong, Z., Yang, J., Vondrick, C., and Ray, B. (2019). Metric learning for adversarial robustness. In *Proceedings of the Conference on Advances in Neural Information Processing Systems*. [arXiv:1909.00900](https://arxiv.org/abs/1909.00900).
- Marcus, G. (2020). The next decade in AI: Four steps towards robust artificial intelligence. [arXiv:2002.06177](https://arxiv.org/abs/2002.06177).
- Menon, A. K., Jayasumana, S., Rawat, A. S., Jain, H., Veit, A., and Kumar, S. (2021). Long-tail learning via logit adjustment. In *Proceedings of the International Conference on Learning Representations*. [arXiv:2007.07314](https://arxiv.org/abs/2007.07314).
- Milletari, F., Navab, N., and Ahmadi, S.-A. (2016). V-net: Fully convolutional neural networks for volumetric medical image segmentation. In *2016 Fourth International Conference on 3D Vision (3DV)*, pages 565–71. doi:[10.1109/3DV.2016.79](https://doi.org/10.1109/3DV.2016.79).
- Ming, Y., Sun, Y., Dia, O., and Li, Y. (2023). How to exploit hyperspherical embeddings for out-of-distribution detection? In *Proceedings of the International Conference on Learning Representations*. <https://openreview.net/forum?id=aEFaE0W5pAd>.
- Mohseni, S., Pitale, M., Yadawa, J., and Wang, Z. (2020). Self-supervised learning for generalizable out-of-distribution detection. In *Proceedings of the AAAI Conference on Artificial Intelligence*, volume 34, pages 5216–23. doi:[10.1609/aaai.v34i04.5966](https://doi.org/10.1609/aaai.v34i04.5966).
- Mu, N. and Gilmer, J. (2019). MNIST-C: A robustness benchmark for computer vision. [arXiv:1906.02337](https://arxiv.org/abs/1906.02337).
- Netzer, Y., Wang, T., Coates, A., Bissacco, A., Wu, B., and Ng, A. Y. (2011). Reading digits in natural images with unsupervised feature learning. In *Proceedings of the Conference on Advances in Neural Information Processing Systems*, Workshop on Deep Learning and Unsupervised Feature Learning.
- Nguyen, A., Yosinski, J., and Clune, J. (2015). Deep neural networks are easily fooled: High confidence predictions for unrecognizable images. In *Proceedings of the IEEE Computer Society Conference on Computer Vision and Pattern Recognition*. [arXiv:1412.1897](https://arxiv.org/abs/1412.1897).
- Pang, T., Xu, K., Dong, Y., Du, C., Chen, N., and Zhu, J. (2020). Rethinking softmax cross-entropy loss for adversarial robustness. In *Proceedings of the International Conference on Learning Representations*. [arXiv:1905.10626](https://arxiv.org/abs/1905.10626).
- Pang, T., Yang, X., Dong, Y., Su, H., and Zhu, J. (2021). Bag of tricks for adversarial training. In *Proceedings of the International Conference on Learning Representations*. [arXiv:2010.00467](https://arxiv.org/abs/2010.00467).
- Panum, T. K., Wang, Z., Kan, P., Fernandes, E., and Jha, S. (2021). Exploring adversarial robustness of deep metric learning. [arXiv:2102.07265](https://arxiv.org/abs/2102.07265).
- Papernot, N., McDaniel, P., Jha, S., Fredrikson, M., Celik, Z. B., and Swami, A. (2016). The limitations of deep learning in adversarial settings. In *IEEE European Symposium on Security and Privacy*. [arXiv:1511.07528](https://arxiv.org/abs/1511.07528).
- Paszke, A., Gross, S., Massa, F., Lerer, A., Bradbury, J., Chanan, G., Killeen, T., Lin, Z., Gimelshein, N., Antiga, L., Desmaison, A., Kopf, A., Yang, E., DeVito, Z., Raison, M., Tejani, A., Chilamkurthy, S., Steiner, B., Fang, L., Bai, J., and Chintala, S. (2019). Pytorch: An imperative style, high-performance deep learning library. In *Proceedings of the Conference on Advances in Neural Information Processing Systems*. [arXiv:1912.01703](https://arxiv.org/abs/1912.01703).
- Ren, J., Yu, C., Sheng, S., Ma, X., Zhao, H., Yi, S., and Li, H. (2020). Balanced meta-softmax for long-tailed visual recognition. In *Proceedings of the Conference on Advances in Neural Information Processing Systems*. [arXiv:2007.10740](https://arxiv.org/abs/2007.10740).
- Rice, L., Wong, E., and Kolter, J. Z. (2020). Overfitting in adversarially robust deep learning. [arXiv:2002.11569](https://arxiv.org/abs/2002.11569).
- Robins, A. (1993). Catastrophic forgetting in neural networks: the role of rehearsal mechanisms. In *Proceedings of the First New Zealand International Two-Stream Conference on Artificial Neural Networks and Expert Systems*, pages 65–8. IEEE.
- Roy, A., Cobb, A., Bastian, N. D., Jalaian, B., and Jha, S. (2022). Runtime monitoring of deep neural networks using top-down context models inspired by predictive processing and dual process theory. In *Proceedings of the AAAI Conference on Artificial Intelligence*.
- Sa-Couto, L. and Wichert, A. (2021). Simple Convolutional-Based Models: Are They Learning the Task or the Data? *Neural Computation*, 33(12):3334–50. doi:[10.1162/neco.a.01446](https://doi.org/10.1162/neco.a.01446).
- Serre, T. (2019). Deep learning: The good, the bad, and the ugly. *Annual Review of Vision Science*, 5(1):399–426. doi:[10.1146/annurev-vision-091718-014951](https://doi.org/10.1146/annurev-vision-091718-014951).
- Spratling, M. W. (2023). A comprehensive assessment benchmark for rigorously evaluating deep learning image classifiers.

- arXiv:2308.04137.
- Szegedy, C., Liu, W., Jia, Y., Sermanet, P., Reed, S., Anguelov, D., Erhan, D., Vanhoucke, V., and Rabinovich, A. (2015). Going deeper with convolutions. In *Proceedings of the IEEE Computer Society Conference on Computer Vision and Pattern Recognition*, pages 1–9. arXiv:1409.4842.
- Szegedy, C., Vanhoucke, V., Ioffe, S., Shlens, J., and Wojna, Z. (2016). Rethinking the inception architecture for computer vision. In *Proceedings of the IEEE Computer Society Conference on Computer Vision and Pattern Recognition*, pages 2818–26. arXiv:1512.00567.
- Tack, J., Yu, S., Jeong, J., Kim, M., Hwang, S. J., and Shin, J. (2022). Consistency regularization for adversarial robustness. In *Proceedings of the AAAI Conference on Artificial Intelligence*. arXiv:2103.04623.
- Tan, J., Wang, C., Li, B., Li, Q., Ouyang, W., Yin, C., and Yan, J. (2020). Equalization loss for long-tailed object recognition. In *Proceedings of the IEEE Computer Society Conference on Computer Vision and Pattern Recognition*. arXiv:2003.05176.
- Tan, M. and Le, Q. V. (2019). Efficientnet: Rethinking model scaling for convolutional neural networks. In *Proceedings of the International Conference on Machine Learning*. arXiv:1905.11946.
- Van Horn, G., Aodha, O. M., Song, Y., Cui, Y., Sun, C., Shepard, A., Adam, H., Perona, P., and Belongie, S. (2018). The inaturalist species classification and detection dataset. In *Proceedings of the IEEE Computer Society Conference on Computer Vision and Pattern Recognition*. arXiv:1707.06642.
- Varrette, S., Cartiaux, H., Peter, S., Kieffer, E., Valette, T., and Olloh, A. (2022). Management of an Academic HPC & Research Computing Facility: The ULHPC Experience 2.0. In *Proc. of the 6th ACM High Performance Computing and Cluster Technologies Conf. (HPCCT 2022)*, Fuzhou, China. Association for Computing Machinery (ACM).
- Vaze, S., Han, K., Vedaldi, A., and Zisserman, A. (2022). Open-set recognition: a good closed-set classifier is all you need? In *Proceedings of the International Conference on Learning Representations*. arXiv:2110.06207.
- Wei, H., Xie, R., Cheng, H., Feng, L., An, B., and Li, Y. (2022). Mitigating neural network overconfidence with logit normalization. In *Proceedings of the International Conference on Machine Learning*, volume 162 of *Proceedings of Machine Learning Research*. arXiv:2205.09310.
- Wightman, R., Touvron, H., and Jégou, H. (2021). Resnet strikes back: An improved training procedure in timm. arXiv:2110.00476.
- Xiao, H., Rasul, K., and Vollgraf, R. (2017). Fashion-MNIST: a novel image dataset for benchmarking machine learning algorithms. arXiv:1708.07747.
- Xie, S., Girshick, R., Dollár, P., Tu, Z., and He, K. (2017). Aggregated residual transformations for deep neural networks. In *Proceedings of the IEEE Computer Society Conference on Computer Vision and Pattern Recognition*. arXiv:1611.05431.
- Xu-Darme, R., Girard-Satabin, J., Hond, D., Incorvaia, G., and Chihani, Z. (2023). Interpretable out-of-distribution detection using pattern identification. <https://hal-cea.archives-ouvertes.fr/cea-03951966>.
- Yang, J., Wang, P., Zou, D., Zhou, Z., Ding, K., Peng, W., Wang, H., Chen, G., Li, B., Sun, Y., Du, X., Zhou, K., Zhang, W., Hendrycks, D., Li, Y., and Liu, Z. (2022). OpenOOD: Benchmarking generalized out-of-distribution detection. In *Proceedings of the Conference on Advances in Neural Information Processing Systems*. arXiv:2210.07242.
- Yang, T., Huang, Y., Xie, Y., Liu, J., and Wang, S. (2023). MixOOD: Improving out-of-distribution detection with enhanced data mixup. *ACM Transactions on Multimedia Computing, Communications, and Applications*. doi:10.1145/3578935.
- Yu, Y. and Xu, C.-Z. (2023). Efficient loss function by minimizing the detrimental effect of floating-point errors on gradient-based attacks. In *Proceedings of the IEEE Computer Society Conference on Computer Vision and Pattern Recognition*, pages 4056–66. doi:10.1109/CVPR52729.2023.00395.
- Yuille, A. L. and Liu, C. (2021). Deep nets: What have they ever done for vision? *International Journal of Computer Vision*, 129:781–802. doi:10.1007/s11263-020-01405-z.
- Zagoruyko, S. and Komodakis, N. (2016). Wide residual networks. In *Proceedings of the British Machine Vision Conference*. arXiv:1605.07146.
- Zenke, F., Poole, B., and Ganguli, S. (2017). Continual learning through synaptic intelligence. In *Proceedings of the International Conference on Machine Learning*, volume 70 of *Proceedings of Machine Learning Research*, pages 3987–95. arXiv:1703.04200.
- Zhang, H., Yu, Y., Jiao, J., Xing, E. P., Ghaoui, L. E., and Jordan, M. I. (2019). Theoretically principled trade-off between robustness and accuracy. In *Proceedings of the International Conference on Machine Learning*. arXiv:1901.08573.
- Zhang, L. H. and Ranganath, R. (2023). Robustness to spurious correlations improves semantic out-of-distribution detection. In *Proceedings of the AAAI Conference on Artificial Intelligence*. arXiv:2302.04132.
- Zhao, L., Teng, Y., and Wang, L. (2024). Logit normalization for long-tail object detection. *International Journal of Computer Vision*, 132:2114–34. doi:10.1007/s11263-023-01971-y.
- Zhu, Q., Zheng, G., and Yan, Y. (2023). Effective out-of-distribution detection in classifier based on PEDCC-loss. *Neural Processing Letters*, 55:1937–49. doi:10.1007/s11063-022-10970-y.
- Zhu, Y., Chen, Y., Li, X., Zhang, R., Xue, H., Tian, X., Jiang, R., Zheng, B., and Chen, Y. (2024). Rethinking out-of-distribution detection from a human-centric perspective. *International Journal of Computer Vision*, 132:4633–50. doi:10.1007/s11263-024-02099-3. arXiv:2211.16778.